The interplay of Dynamical Systems Analysis and Group Theory

P M Tchepmo Djomegni

THE INTERPLAY OF DYNAMICAL SYSTEMS ANALYSIS AND GROUP THEORY

P M Tchepmo Djomegni

This dissertation is submitted to the School of Mathematical Sciences, Faculty of Science and Agriculture, University of KwaZulu-Natal, Durban, in fulfillment of the requirements for the degree of Master in Science.

December 2011

As the candidate's supervisor, I have approved this dissertation for submission.

Signed: Professor K S Govinder December 2011

Abstract

We investigate the relationship between the Dynamical Systems analysis and the Lie Symmetry analysis of ordinary differential equations. We undertake this investigation by looking at a relativistic model of self-gravitating charged fluids. Specifically we look at the impact of specific parameters obtained from Lie Symmetries analysis on the qualitative behaviour of the model. Steady states, stability and possible bifurcations are explored.

Declaration

I declare that the contents of this dissertation are original except where due reference has been made. It has not been submitted before for any degree to any other institution.

P M Tchepmo Djomegni

December 2011

Declaration 1 - Plagiarism

I, Patrick Mimphis Tchepmo Djomegni, declare that

1. The research reported in this thesis, except where otherwise indicated, is my original research.
2. This thesis has not been submitted for any degree or examination at any other university.
3. This thesis does not contain other persons data, pictures, graphs or other information, unless specifically acknowledged as being sourced from other persons.
4. This thesis does not contain other persons' writing, unless specifically acknowledged as being sourced from other researchers. Where other written sources have been quoted, then:
    a. Their words have been re-written but the general information attributed to them has been referenced
    b. Where their exact words have been used, then their writing has been placed in italics and inside quotation marks, and referenced.
5. This thesis does not contain text, graphics or tables copied and pasted from the Internet, unless specifically acknowledged, and the source being detailed in the thesis and in the References sections.

Signed

Acknowledgments

First, I thank God for his guidance and company, for strength and courage he has provided to complete this study.

I am deeply thankful to my supervisor, Professor K S Govinder, for his guidance and help, his patience and encouragement. I also thank him for introducing me to research, and to the use of software packages Mathematica, Maple and LaTeX. In addition to his excellent coaching, his financial support allowed me to enjoy my task.

My gratitude to the School of Mathematical Sciences for financial support and diverse facilities.

I am indebted to my father Hubert and my deceased mother Emilienne for their love, encouragements and their moral, spiritual and financial support throughout my education. I also thank my aunt Marthe for her encouragements and advice, the family Kwawou for their spiritual support, and my lovely friend Naomie for her emotional support.

I am also grateful to Emile, Bienvenue, Rodrigue and Natacha for their advice, support and spiritual guidance, and my gratitude to Keith for reviewing my work, and to Elyzee for her friendship and support.

To God be the Glory.

Dedication

To my dear father Hubert and my deceased mother Emilienne

To my lovable brothers Junior, Bruno, and sisters Agnes, Judith, Ariane

To my beloved Naomie

"Only be strong and very courageous, faithfully doing everything in the teachings that my servant Moses commanded you. Dont turn away from them. Then you will succeed wherever you go." Joshua 1:7.

Contents

Chapter 1

Introduction

Most of the real word problems (in biology, finance, economics, industry, etc.), and many fundamental laws of physics and chemistry are formulated as differential (or difference) equations. A variety of methods for solving differential equations (analytically and numerically) have been developed. Around 1870, Marius Sophie Lie realized that many of these methods could be unified using group theory; he thus introduced the notion of Lie groups [22]. Lie symmetries play an important role in the modern approach for solving differential equations. We use Lie symmetries to reduce the number of independent variables of PDEs, to reduce the order of ODEs, to construct the types of equations that admit a prescribed group of transformations, and to determine first integrals [20].

Despite the efforts made to extend this notion, most nonlinear differential equations are impossible to solve explicitly. For example, it was eventually realized that equations describing the motion of the three-body problem (sun, earth and moon) was impossible to solve analytically [24]. In the late 1800s, Poincaré introduced a new point of view that emphasized qualitative rather than quantitative questions. For example, instead of asking for the exact positions of the planets at all times, he asked "Is the solar system stable forever, or will some planets eventually fly off to infinity?" [24]. This approach led to a new field of study called dynamical systems.

A dynamical system is specified by a state vector $x \in \mathbb{R}^n$ and a function $f : \mathbb{R}^n \to \mathbb{R}^n$ which describes how the system evolves over time [23]. Important goals are to describe the steady

state of the system, to look at the periodic points, and investigate possible chaotic behaviour. There are two kinds of dynamical systems: continuous and discrete. We are interested in the continuous type. Our goal is to investigate the interplay between Lie symmetries analysis and dynamical systems analysis.

1.1 Some simple models

1.1.1 Malthusian growth model

Sometimes called **simple exponential growth**, this model is based on a constant rate of compound interest. It is given by [6, p 11–12]

$$\dot{N} = rN, \tag{1.1}$$

where N is the population species, and r the difference between birth and death rates.

$N = 0$ is the steady state; it is stable when $r < 0$, and unstable when $r > 0$. The unstable state corresponds to an exponential growth, while the stable state to a disappearance of the species. This result is clearly illustrated when we consider the solution of (1.1), given by

$$N(t) = N_0 e^{rt}, \tag{1.2}$$

where N_0 is the population size at time $t = 0$. Thus we have exponential growth when $r > 0$ and exponential decay when $r < 0$. The behaviour is shown in Figure 1.1.

1.1.2 The logistic equation

Considering overcrowding and limited resources, such exponential growth (Figure 1.1(a)) cannot go on forever. Biologists assumed that the environment has an intrinsic carrying capacity K [19]. Thus for a population larger than K, this size experience heightened death rates. This led to the logistic equation. This equation was first suggested by Verhulst in 1838 to describe the growth of human populations [24]. It is given by

$$\dot{N} = rN\left(1 - \frac{N}{K}\right), \tag{1.3}$$

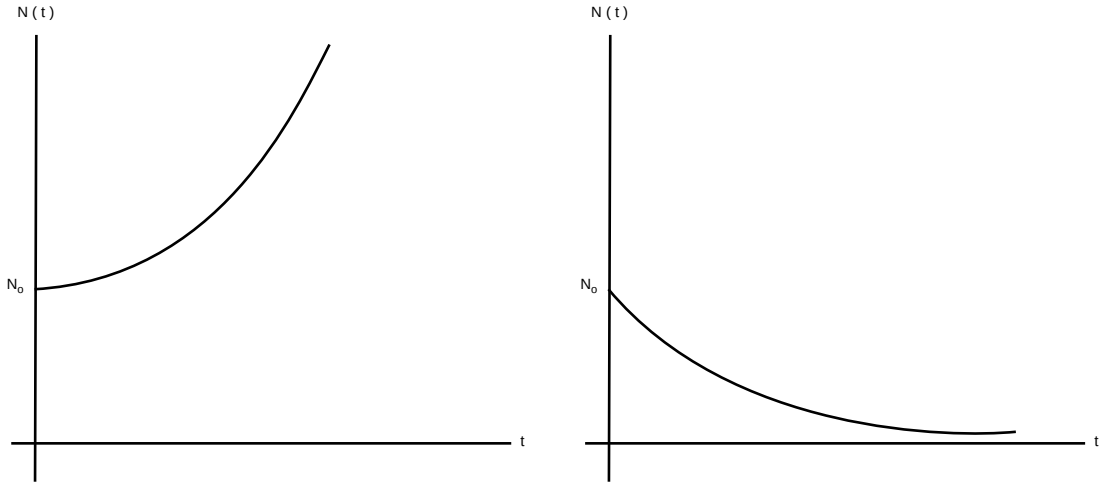

(a) Case $r > 0$ (b) Case $r < 0$

Figure 1.1: Changes in population size $N(t)$.

where $r\left(1 - \dfrac{N}{K}\right)$ is per capita growth rate, with $r > 0$ [19]. There are two steady states: the state $N = 0$ which is unstable, and the state $N = K$ which is stable. For the initial condition $N(0) = N_0$, (1.3) is solved explicitly as follows

$$N(t) = \frac{N_0}{\dfrac{N_0}{K} + \left(1 - \dfrac{N_0}{K}\right) e^{-rt}}. \tag{1.4}$$

Thus

$$\lim_{t\to\infty} N(t) = K, \qquad \lim_{K\to\infty} N(t) = N_0 e^{rt}. \tag{1.5}$$

Consequently, for a large space ($K \to \infty$), we have the exponential growth model. The graphical representation of solution $N(t)$ is shown in Figure 1.2. Note that different curves correspond to different initials conditions.

1.2 Outline

As we have previously mentioned, nonlinear equations are difficult to solve analytically in general. To reduce the equation in the simplest way, sometimes we need to seek constraints to get

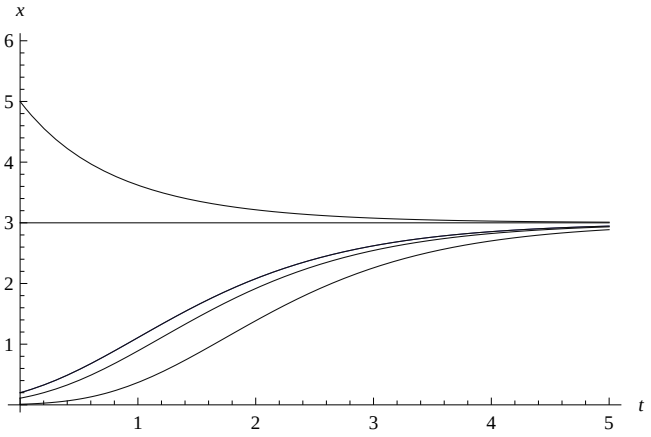

Figure 1.2: Changes in population size predicted by the logistic equation ($K = 3$).

Lie symmetries, or additional Lie symmetries. The aim of this dissertation is to investigate the impact of those constraints obtained from Lie symmetries analysis on the qualitative behaviour of the system. First we will give an overview of dynamical systems analysis in two dimensional flow in chapter 2, then briefly introduce Lie symmetry analysis (of ordinary differential equations) in chapter 3. In chapter 4 we undertake an investigation by looking at a relativistic model of self-gravitating charged fluids; a full dynamical system analysis is explored. The main discussion is presented in chapter 5. Most of our figures are plotted in Mathematica [26], using DynPac [7], and some in Maple [18].

Chapter 2

Overview of Dynamical Systems analysis

2.1 Introduction

In this chapter, we are interested in two-dimensional autonomous systems

$$\begin{aligned} x' &= f(x, y) \\ y' &= g(x, y), \end{aligned} \tag{2.1}$$

where f and g are smooth real-valued functions and x and y are real-valued functions of time t. Here the notation prime denotes differentiation with respect to t. We assume that the solutions of the system exist.

A solution of (2.1) is a pair of functions $x(t)$ and $y(t)$ satisfying the system (2.1), i.e,

$$\begin{aligned} x'(t) &= f(x(t), y(t)) \\ y'(t) &= g(x(t), y(t)). \end{aligned} \tag{2.2}$$

If we construct a space with coordinates x and y, then the solutions $(x(t), y(t))$ correspond to the points moving along a curve in this space [24]. This curve is called a **trajectory**, and the space is called the **phase space** (or **phase plane** as we are in two dimension).

Our goal is to describe the qualitative behaviour of the system (2.1) in the phase plane, especially near the stationary conditions, and then represent the trajectories. We also explore stability and bifurcations. We first present some basic definitions.

Definition 2.1.1. ***Equilibrium points*** *of system (2.1) are the solutions of the equations [3]*

$$x' = 0 \tag{2.3}$$

and

$$y' = 0. \tag{2.4}$$

■

They represent stationary conditions for the dynamics of a system.

Definition 2.1.2. *An equilibrium point is* ***stable*** *if all trajectories that start sufficiently close remain close for all time (Lyapunov stable), and approach it as $t \to \infty$ (attractor) [24].* ■

An equilibrium point is **unstable** if it is not stable.

2.2 Two dimensional linear systems

Here we only consider linear systems. Thus we take system (2.1) to be

$$\begin{pmatrix} x' \\ y' \end{pmatrix} = A \begin{pmatrix} x \\ y \end{pmatrix}, \tag{2.5}$$

where A is a real matrix. The analysis is focused on the nature and stability of the equilibrium points in the phase plane. Let λ_1 and λ_2 be the eigenvalues of the matrix A in (2.5).

2.2.1 $\lambda_1 \neq \lambda_2$

In this case the matrix A in (2.5) is diagonalisable [1]. Thus we can find two square matrices P and D such that $A = P^{-1}DP$, with P an invertible matrix formed by the eigenvectors

associated with the eigenvalues, and D a diagonal matrix formed by the eigenvalues λ_1 and λ_2. Thus system (2.5) becomes

$$\begin{pmatrix} x' \\ y' \end{pmatrix} = \left(P^{-1}DP\right) \begin{pmatrix} x \\ y \end{pmatrix}. \tag{2.6}$$

In order to reduce (2.5) to an uncoupled linear system, we define the linear transformation [21]

$$\begin{pmatrix} u \\ v \end{pmatrix} = P \begin{pmatrix} x \\ y \end{pmatrix}. \tag{2.7}$$

Differentiating, we obtain

$$\begin{pmatrix} u' \\ v' \end{pmatrix} = P \begin{pmatrix} x' \\ y' \end{pmatrix} = P\left(P^{-1}DP\right) \begin{pmatrix} x \\ y \end{pmatrix} = DP \begin{pmatrix} x \\ y \end{pmatrix} = D \begin{pmatrix} u \\ v \end{pmatrix}. \tag{2.8}$$

Thus (2.5) is transformed to the system

$$\begin{pmatrix} u' \\ v' \end{pmatrix} = \begin{pmatrix} \lambda_1 & 0 \\ 0 & \lambda_2 \end{pmatrix} \begin{pmatrix} u \\ v \end{pmatrix}. \tag{2.9}$$

Therefore

$$u' = \lambda_1 u \tag{2.10}$$

$$v' = \lambda_2 v. \tag{2.11}$$

Using the initials conditions $u(0) = u_0$ and $v(0) = v_0$, (2.10)–(2.11) admits as solution

$$u = u_0 e^{\lambda_1 t} \tag{2.12}$$

$$v = v_0 e^{\lambda_2 t}. \tag{2.13}$$

From (2.10)–(2.11) if $\lambda_1 \neq 0$, then

$$\frac{v'}{v} = \frac{\lambda_2}{\lambda_1}\frac{u'}{u}. \tag{2.14}$$

Thus

$$v = ku^{\gamma}, \tag{2.15}$$

where k is a constant, and $\gamma = \dfrac{\lambda_2}{\lambda_1}$.

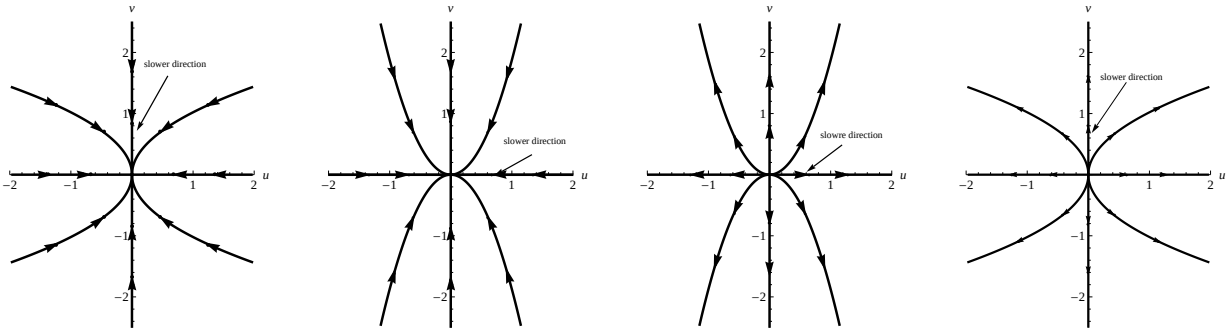

(a) $\lambda_1 < 0, \lambda_2 < 0$, with $\lambda_1 < \lambda_2$

(b) $\lambda_1 < 0, \lambda_2 < 0$, with $\lambda_1 > \lambda_2$

(c) $\lambda_1 > 0, \lambda_2 > 0$, with $\lambda_1 < \lambda_2$

(d) $\lambda_1 > 0, \lambda_2 > 0$, with $\lambda_1 > \lambda_2$

Figure 2.1: Stable and unstable nodes.

Assume $(\lambda_1, \lambda_2) \in \mathbb{R}$

i) When $\lambda_1 < 0$ and $\lambda_2 < 0$, $u(t)$ and $v(t)$ in (2.12)–(2.13) decay exponentially and the trajectories approach the origin. Therefore the origin is a **stable node**.

- For $\lambda_1 < \lambda_2$, $u(t)$ decays more rapidly than $v(t)$. Then the trajectories approach the origin tangent to the *slower direction*, the v-axis.

– For $\lambda_1 > \lambda_2$, the trajectories approach the origin tangent to the u-axis, which is now the slower direction.

The phase portrait is shown in Figures 2.1(a)–2.1(b).

ii) When $\lambda_1 > 0$ and $\lambda_2 > 0$, $u(t)$ and $v(t)$ increase exponentially. The trajectories move away from the origin. Hence, the origin is an **unstable node**.

Contrary to the previous case, if $\lambda_1 < \lambda_2$, then $v(t)$ increases more faster than $u(t)$. Hence the u-axis is the slower direction. But if $\lambda_1 > \lambda_2$, the v-axis is the slower direction. The above two cases are illustrated in Figures 2.1(c)–2.1(d).

iii) When λ_1 and λ_2 have opposite signs (say $\lambda_1 > 0$ and $\lambda_2 < 0$) then $u(t)$ increases and $v(t)$ decreases exponentially. Thus the origin is unstable due to the exponential growth in the u-direction; therefore it is a **saddle point**.

The v-axis is called the stable manifold of the saddle point, defined as the set of initial

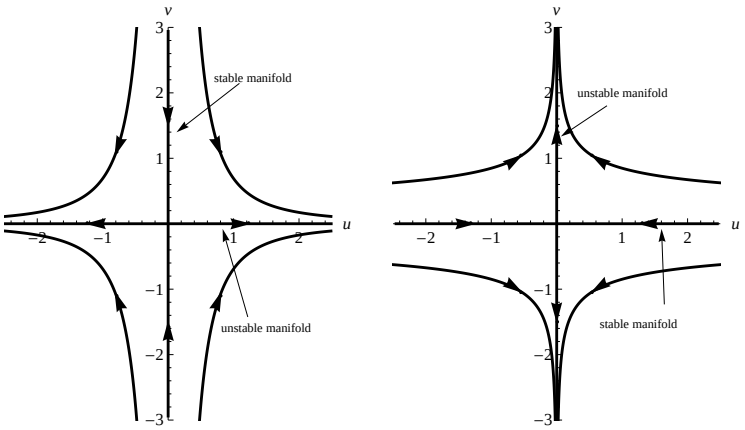

(a) $\lambda_1 > 0$ and $\lambda_2 < 0$ (b) $\lambda_1 < 0$ and $\lambda_2 > 0$

Figure 2.2: Saddle points at the origin.

conditions (u_0, v_0) such that $v(t) \to 0$ as $t \to \infty$. The u-axis is called the unstable manifold [24] (see Figure 2.2).

iv) If one eigenvalue is zero (say $\lambda_1 = 0$), then the origin is a **non isolated** equilibrium point; we have a whole line of equilibrium points – the u-axis.

- For $\lambda_2 < 0$, the equilibrium points are **neutrally stable** (they are Lyapunov stable, but not attractors).
- For $\lambda_2 > 0$, the equilibrium points are **unstable**.

Similar results are obtained if the roles of λ_1 and λ_2 are reversed. The phase portraits for these cases are shown in Figure 2.3.

Assume $\left(\lambda_1, \lambda_2 = \bar{\lambda}_1\right) \in \mathbb{C}$

Let

$$\lambda_1 = \alpha + i\beta, \tag{2.16}$$

where α and β are real (with $\beta \neq 0$), and $\bar{\lambda}_1$ is the complex conjugate of λ_1. The origin is the only equilibrium point, and equation (2.10) is reduced to

$$u' = (\alpha + i\beta)u. \tag{2.17}$$

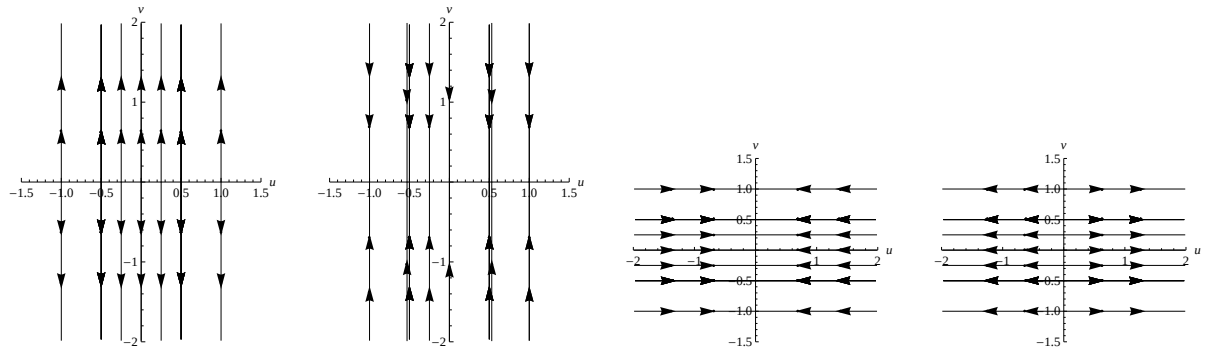

(a) $\lambda_2 > 0$, $\lambda_1 = 0$ (b) $\lambda_2 < 0$, $\lambda_1 = 0$ (c) $\lambda_1 < 0$, $\lambda_2 = 0$ (d) $\lambda_1 > 0$, $\lambda_2 = 0$

Figure 2.3: Whole lines of equilibrium points

As u is complex, we consider the polar form

$$u = re^{i\theta}, \tag{2.18}$$

with r a non zero real, and $\theta \in [0, 2\pi]$. Differentiating (2.18) yields

$$u' = r'e^{i\theta} + ir\theta' e^{i\theta} = (r' + ir\theta')e^{i\theta}. \tag{2.19}$$

Substituting u in (2.17) from (2.18):

$$(r' + ir\theta')e^{i\theta} = (\alpha + i\beta)re^{i\theta}. \tag{2.20}$$

This implies that

$$r' + ir\theta' = \alpha r + ir\beta. \tag{2.21}$$

Thus, we obtain the following system in polar coordinates

$$r' = \alpha r \tag{2.22}$$

$$\theta' = \beta. \tag{2.23}$$

This system admits as solution

$$r = r_0 e^{\alpha t} \tag{2.24}$$

and

$$\theta = \beta t + \theta_0, \tag{2.25}$$

where r_0 and θ_0 are initial conditions. The phase portrait is given by sketching the graph of the polar system (2.24)–(2.25).

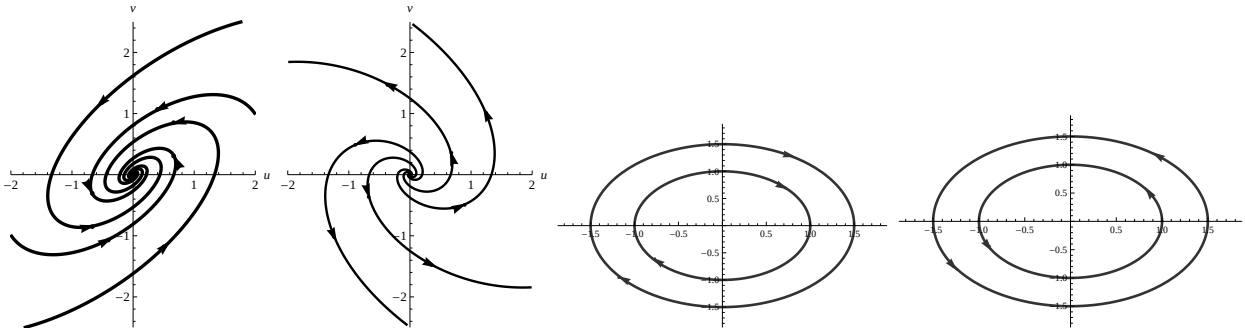

(a) $\alpha < 0$ (b) $\alpha > 0$ (c) $\alpha = 0$ and $\beta < 0$ (d) $\alpha = 0$ and $\beta > 0$

Figure 2.4: Spirals and centres at the origin

i) If $\alpha \neq 0$, (2.24)–(2.25) yield

$$r = r_0 e^{\alpha\left(\frac{\theta-\theta_0}{\beta}\right)} = ae^{b\theta}. \tag{2.26}$$

This is the equation of a logarithmic spiral [8]. Therefore the origin is a **spiral**. It is a **stable spiral** when $\alpha < 0$ (due to the exponential decay in (2.24)), and an **unstable spiral** when $\alpha > 0$.

ii) If $\alpha = 0$, the radius in (2.24) is *constant*. As a result the origin is a **centre**. The direction of the vector fields is given by the sign of β. When $\beta > 0$, the flow is counter-clockwise, and when $\beta < 0$, it is clockwise.

The above behaviour is shown in Figure 2.4.

2.2.2 $\lambda_1 = \lambda_2 = \lambda$

Hence we have two possibilities: either there are two independent eigenvectors associated with λ, or there is only one.

If there are two independent eigenvectors, then the matrix A is diagonalisable [1]. As in §2.2.1:

i) When $\lambda \neq 0$, (2.15) becomes

$$v = ku. \tag{2.27}$$

Thus all trajectories are **straight lines** through the origin. Therefore the origin is a **star**.

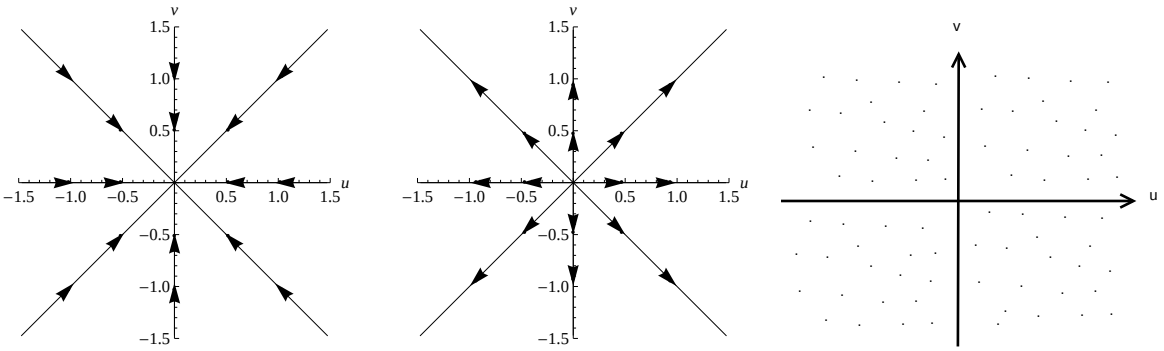

(a) Case $\lambda < 0$ (b) Case $\lambda > 0$ (c) Case $\lambda = 0$

Figure 2.5: Stars and whole plane of equilibrium points

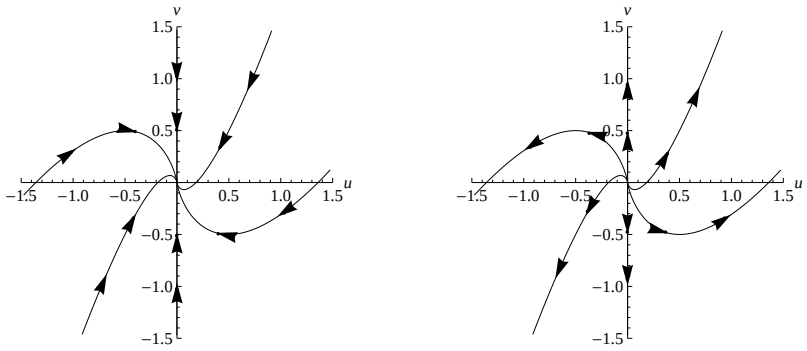

(a) Case $\lambda < 0$ (b) Case $\lambda > 0$

Figure 2.6: Degenerate node

It is an **unstable star** if $\lambda > 0$ (exponential growth in (2.12)–(2.13)), and a **stable star** if $\lambda < 0$ (see Figures 2.5(a)–2.5(b)).

ii) When $\lambda = 0$, (2.10)–(2.11) yields

$$u' = v' = 0. \tag{2.28}$$

Thus the whole plane is filled with the equilibrium points. The phase portrait is shown in Figure 2.5(c).

On the other hand, if there is only one eigenvector associated with λ, then the origin is a **degenerate node** [24]. The node is stable when $\lambda < 0$, and unstable when $\lambda > 0$. The behaviour is shown in Figure 2.6.

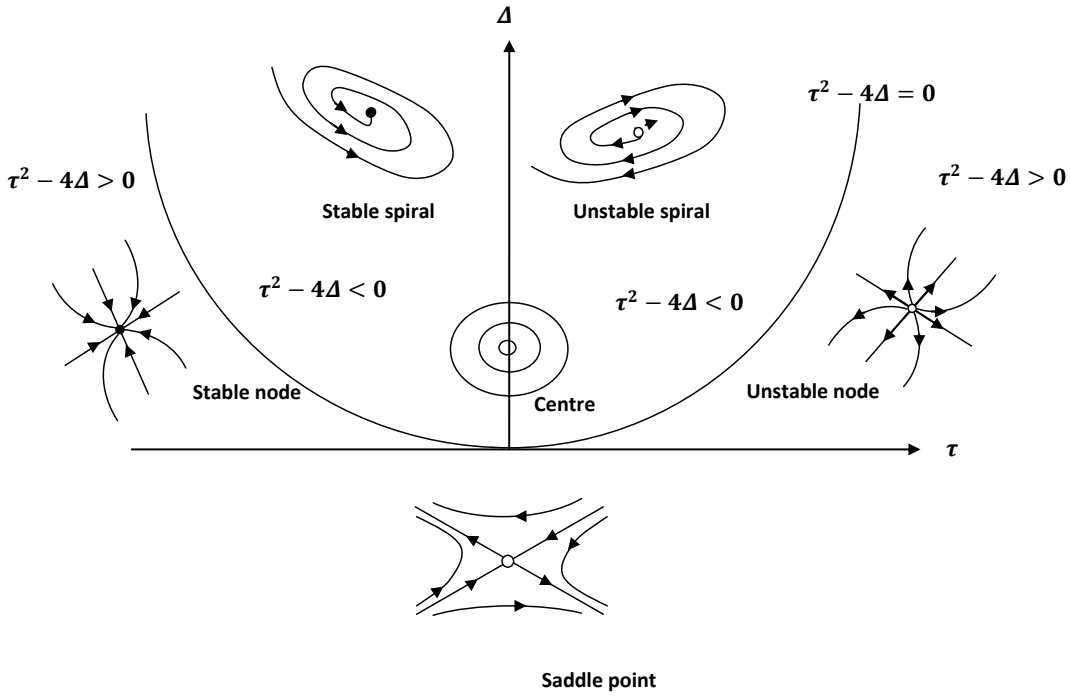

Figure 2.7: Diagram of the classification of equilibrium points [24].

2.2.3 Classification of linear systems

This classification applies to all two-dimensional linear systems. If λ_1 and λ_2 are the eigenvalues of the matrix A, and if τ and Δ are respectively the trace and the determinant of the matrix A, then

$$\lambda_{1,2} = \frac{1}{2}\left(\tau \pm \sqrt{\tau^2 - 4\Delta}\right), \quad \Delta = \lambda_1\lambda_2, \quad \tau = \lambda_1 + \lambda_2. \tag{2.29}$$

We can describe the type and stability of the equilibrium points in a single diagram as shown in Figure 2.7. The interpretation of this diagram is given in Table 2.1, with (x^*, y^*) an equilibrium point.

$\Delta < 0$	λ_1 and λ_2 are real with the opposite signs; hence (x^*, y^*) is a **saddle point**.
$\Delta > 0$	If $\tau = 0$, at (x^*, y^*) we have a **centre**. This is a borderline case. However if $\tau \neq 0$, (x^*, y^*) is **stable** when $\tau < 0$, and **unstable** when $\tau > 0$. In that case: i) If $\tau^2 - 4\Delta > 0$, λ_1 and λ_2 are real with the same sign. Therefore (x^*, y^*) is a **node**. ii) If $\tau^2 - 4\Delta < 0$, λ_1 and λ_2 are complex conjugates. Therefore (x^*, y^*) is a **spiral**. iii) If $\tau^2 - 4\Delta = 0$, then $\lambda_1 = \lambda_2$. - If there is only one eigenvector associated to λ_1, then (x^*, y^*) is a **degenerate node**. - If there are two independents eigenvectors, then we have a **star**. Degenerate nodes and stars live on the parabola $\tau^2 - 4\Delta = 0$. We are in a borderline case, though the stability is robust.
$\Delta = 0$	We are in a borderline case, at least one eigenvalue is zero. Thus (x^*, y^*) is a **non isolated** equilibrium point. - If $\lambda_1 = \lambda_2 = 0$, then $A = 0$. Thus we have a **whole plane** of equilibrium points. - If $\lambda_1 \neq 0$ or $\lambda_2 \neq 0$, we have a **whole axis** of equilibrium points, and at each point, the trajectories are straights lines.

Table 2.1: Classification of equilibrium points.

2.3 Nonlinear systems

Most scientific problems are nonlinear, and nonlinear problems are much harder to analyse than linear. The essential difference is that linear systems can be broken down into parts [24]. Each part can be solved separately and finally combined to get the answer (one typical example is shown in the previous section, where system (2.5) was transformed to (2.9)). To establish the nonlinear stability at an equilibrium point, we need to examine if any small perturbation of the system away from the equilibrium point eventually returns to the fixed point after a sufficiently long time [9]. The most expeditious way of establishing this is by investigating the corresponding linearized system because (as we will see below) around some particular fixed points, the behaviour or the stability of the nonlinear system is approximately the same as the one predicted by the linearized system.

2.3.1 Linearisation

We now consider the fully nonlinear system (2.1), and we suppose that (x^*, y^*) is an equilibrium point, i.e,

$$f(x^*, y^*) = 0, \tag{2.30}$$

and

$$g(x^*, y^*) = 0. \tag{2.31}$$

For a small perturbation near (x^*, y^*), let [24]

$$u = x - x^*, \tag{2.32}$$

and

$$v = y - y^*. \tag{2.33}$$

Differentiating equation (2.32) (since x^* is constant) we obtain

$$u' = x' = f(x, y) = f(x^* + u, y^* + v). \tag{2.34}$$

Using the Taylor series expansion about (x^*, y^*) and the fact that (x^*, y^*) is an equilibrium point, (2.34) becomes

$$\begin{aligned} u' &= f(x^*, y^*) + \left(u\frac{\partial f}{\partial x} + v\frac{\partial f}{\partial y} \right)(x^*, y^*) + O\left(u^2, v^2, uv\right) \\ &= \left(u\frac{\partial f}{\partial x} + v\frac{\partial f}{\partial y} \right)(x^*, y^*) + O\left(u^2, v^2, uv\right). \end{aligned} \tag{2.35}$$

The notation $O\left(u^2, v^2, uv\right)$ denotes terms of order two or higher in u and v. Since u and v are small, these terms are much smaller.

Similarly we find

$$v' = \left(u\frac{\partial g}{\partial x} + v\frac{\partial g}{\partial y} \right)(x^*, y^*) + O\left(u^2, v^2, uv\right). \tag{2.36}$$

Hence the pertubation (u, v) evolves according to

$$\begin{pmatrix} u' \\ v' \end{pmatrix} = \begin{pmatrix} \frac{\partial f}{\partial x}(x^*, y^*) & \frac{\partial f}{\partial y}(x^*, y^*) \\ \frac{\partial g}{\partial x}(x^*, y^*) & \frac{\partial g}{\partial x}(x^*, y^*) \end{pmatrix} \begin{pmatrix} u \\ v \end{pmatrix} + O\left(u^2, v^2, uv\right), \tag{2.37}$$

or

$$\begin{pmatrix} u' \\ v' \end{pmatrix} = A \begin{pmatrix} u \\ v \end{pmatrix}. \tag{2.38}$$

when the higher order terms are ignored. The matrix

$$A = \begin{pmatrix} \frac{\partial f}{\partial x}(x^*, y^*) & \frac{\partial f}{\partial y}(x^*, y^*) \\ \frac{\partial g}{\partial x}(x^*, y^*) & \frac{\partial g}{\partial x}(x^*, y^*) \end{pmatrix} \tag{2.39}$$

is called the **Jacobian matrix** at the equilibrium point (x^*, y^*), and (2.38) is the **linearization** of system (2.1).

2.3.2 Stability analysis

Andronov *et al* [2] proved that it is safe to neglect the terms of order two in (2.37) as long as the stability at an equilibrium point predicted by the linearized system is not one of the borderline cases discussed in Table 2.1. Therefore if the linearized system predicts a saddle point, a node, or a spiral, then the equilibrium point really is a saddle point, a node, or a spiral for the nonlinear system.

In the case where the linearized system predicts a star or a degenerate node, the stability of the full nonlinear system at the corresponding point is the same as the one predicted by the linearized system [24]. However, the nature of the equilibrium point could change. For example, a stable star may be changed to a stable node or stable spiral, but not to an unstable node or unstable spiral.

Centres are more delicate. There are many ways to pursue the analysis. We can use for example center manifold theory, conservative systems approach, reversible systems, limit cycles, etc [24, 10]. In this study, we are interested in reversible systems.

Definition 2.3.1. *We say the system (2.1) is* ***reversible*** *if the function f is odd in y, and g is even in y [24] (i.e, $f(x,-y) = -f(x,y)$ and $g(x,-y) = g(x,y)$).* ■

Theorem 2.3.2. *If a system is reversible and the linear analysis at an equilibrium point predicts a centre, then sufficiently close to the point, all trajectories are closed curves [24]. Thus the equilibrium point is a* ***nonlinear centre****.* ■

2.4 Bifurcations

Bifurcations occur when a small smooth change made to a parameter value (commonly called a bifurcation parameter) of a system, causes a sudden qualitative change or topological change (for example trajectories could extend out to an arbitrary large distance) in its behaviour [4]. They are divided into two principal classes: local bifurcations and global bifurcations. We will focus on local bifurcations, especially saddle-node, transcritical and pitchfork bifurcations.

2.4.1 Saddle-node bifurcation

This is a local bifurcation in which two equilibrium points collide and vanish [25]. Consider the prototypical example defined as [24]

$$\begin{aligned} x' &= \mu + x^2 \\ y' &= -y. \end{aligned} \tag{2.40}$$

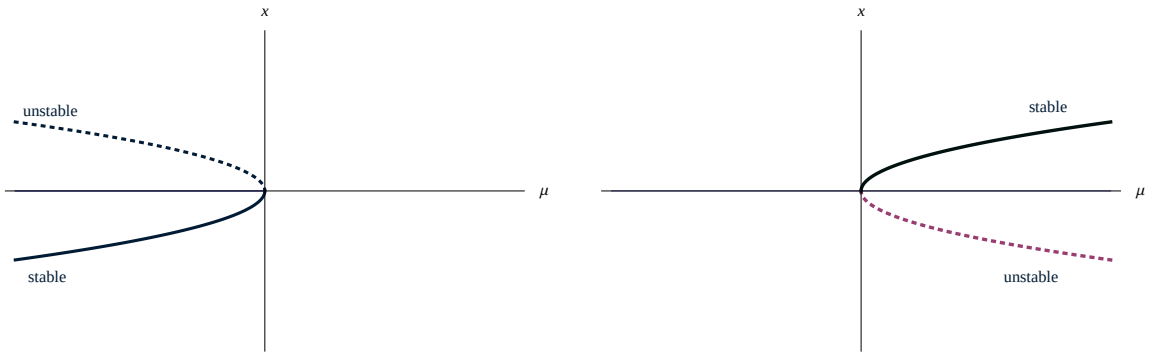

(a) Saddle-node bifurcation

(b) Blue sky bifurcation

Figure 2.8: Saddle-node bifurcation diagram.

When $\mu < 0$, there are two equilibrium points, $(-\sqrt{-\mu}, 0)$ which is stable, and $(\sqrt{-\mu}, 0)$ which is unstable. When $\mu = 0$ the equilibrium points coalesce, and then disappear when $\mu > 0$. This is called a saddle-node bifurcation, with μ as the bifurcation parameter. The bifurcation diagram is shown in Figure 2.8(a).

There is a particular type of saddle-node bifurcation where an equilibrium point suddenly appears, and then splits into two equilibrium points. Abraham and Shaw [24] invented a new terminology for this phenomena, called a **blue sky bifurcation**. For example consider [24]

$$\begin{aligned} x' &= \mu - x^2 \\ y' &= -y. \end{aligned} \tag{2.41}$$

There is no equilibrium point when $\mu < 0$; one equilibrium point appears when $\mu = 0$, and then splits into two when $\mu > 0$; a blue sky bifurcation occurs. This is illustrated in Figure 2.8(b).

2.4.2 Transcritical bifurcation

This is a particular kind of local bifurcation in which an equilibrium point exists for all values of parameters, and is never destroyed. However, the stability is exchanged when the points collide [24]. Consider

$$\begin{aligned} x' &= \mu x - x^2 \\ y' &= -y. \end{aligned} \tag{2.42}$$

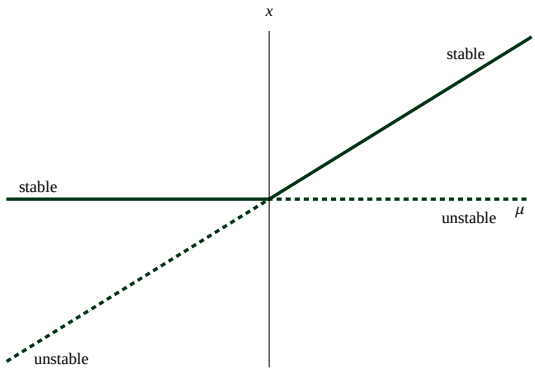

Figure 2.9: Transcritical bifurcations diagram

There are two equilibrium points $(0, 0)$ and $(\mu, 0)$ for $\mu \neq 0$, and only one, the origin, for $\mu = 0$. When $\mu < 0$ the origin is a stable node whereas $(\mu, 0)$ is an unstable saddle point. When $\mu = 0$ the points fuse to one. When $\mu > 0$, $(\mu, 0)$ is now a stable node whereas the origin becomes unstable. This is called a transcritical bifurcation (see Figure 2.9).

2.4.3 Pitchfork bifurcation

This bifurcation is common in physical problems that have a symmetry. The equilibrium points tend to appear and disappear in symmetrical pairs [24]. There are two types of pitchfork bifurcations: supercritical and subcritical.

Supercritical pitchfork bifurcation

The canonical example is [24]

$$\begin{aligned} x' &= \mu x - x^3 \\ y' &= -y. \end{aligned} \tag{2.43}$$

When $\mu \leq 0$ the origin is the only equilibrium point, and when $\mu > 0$ two symmetrical pairs of equilibrium points $(-\sqrt{\mu}, 0)$ and $(\sqrt{\mu}, 0)$ appear – a supercritical pitchfork bifurcation occurs. The bifurcation diagram is shown in Figure 2.10(a).

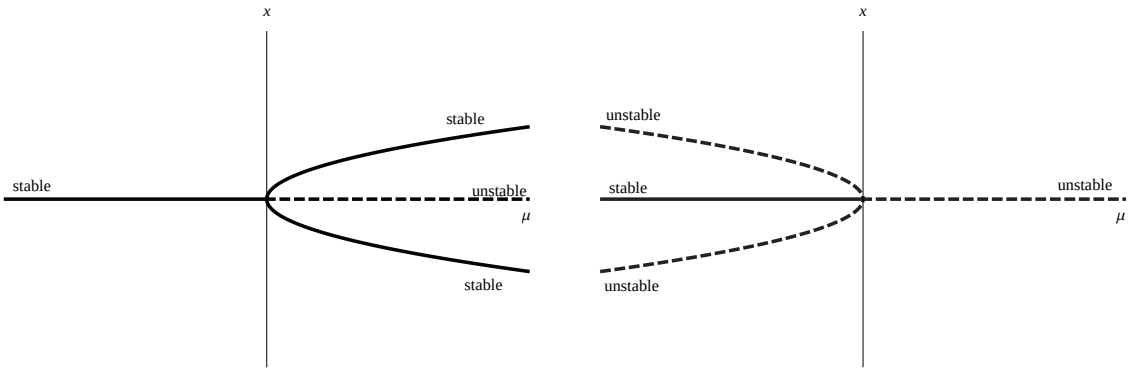

(a) Supercritical pitchfork bifurcation (b) Subcritical pitchfork bifurcation

Figure 2.10: Pitchfork bifurcation diagram.

Subcritical pitchfork bifurcation

The canonical example is [24]

$$\begin{aligned} x' &= \mu x + x^3 \\ y' &= -y. \end{aligned} \tag{2.44}$$

Compared to the supercritical bifurcation, the pitchfork is inverted. The stability analysis shows that $(-\sqrt{-\mu}, 0)$ and $(\sqrt{-\mu}, 0)$ are unstable whereas the origin is stable when $\mu < 0$. However, when $\mu \geq 0$ $(-\sqrt{-\mu}, 0)$ and $(\sqrt{-\mu}, 0)$ disappear and the origin becomes unstable. This is a subcritical pitchfork bifurcation (see Figure 2.10(b)).

Chapter 3

Lie Symmetry analysis of an Ordinary Differential Equation

We present an overview of Lie symmetry analysis applied to ordinary differential equations. To illustrate different aspects of the theory, we consider one of the equations obtained by Kweyama *et al* [15] in the study of the behaviour of spherically symmetric charged fluids in general relativity.

3.1 Introductory concepts

Definition 3.1.1. *Let* $\mathbf{x} = (x_1, x_2, ..., x_n)$ *lie in region* $D \subset \mathbb{R}^n$. *The set of transformations [5, p 36]*

$$\mathbf{x}^* = X(\mathbf{x},\varepsilon),$$

defined for each $\mathbf{x}$ *in* D *and parameter* ε *in set* $S \subset \mathbb{R}$, *with* $\phi(\varepsilon, \delta)$ *defining a law of composition of parameters* ε *and* δ *in* S, *forms a* ***one-parameter group of transformations*** *on* D *if the following hold:*

i) For each ε *in* S *the transformations are one-to-one onto* D.

ii) S with the law of composition ϕ forms a group.

iii) For each $\mathbf{x}$ *in* D, $\mathbf{x}^* = \mathbf{x}$ *when* $\varepsilon = \varepsilon_0$ *corresponds to the identity* e, *i.e.*,

$$\mathbf{x} = X(\mathbf{x},\varepsilon_0).$$

iv) If $\mathbf{x}^* = X(\mathbf{x},\varepsilon)$, $\mathbf{x}^{**} = X(\mathbf{x}^*,\delta)$, *then*

$$\mathbf{x}^{**} = X(\mathbf{x},\phi(\varepsilon,\delta)).$$

■

Considering the one-parameter group of transformation

$$x^* = \phi\left(x, y, \varepsilon\right), \quad y^* = \Phi\left(x, y, \varepsilon\right), \tag{3.1}$$

the Taylor series expansions in a neighborhood of $\varepsilon = 0$, lead to [12]

$$x^* \approx x + \varepsilon\xi(x, y) \tag{3.2}$$

$$y^* \approx y + \varepsilon\eta(x, y), \tag{3.3}$$

where

$$\xi(x, y) = \left.\frac{dx^*}{d\varepsilon}\right|_{\varepsilon=0} \tag{3.4}$$

and

$$\eta(x, y) = \left.\frac{dy^*}{d\varepsilon}\right|_{\varepsilon=0} \tag{3.5}$$

and we have ignored higher order terms in ε. We call (3.2)–(3.3) the infinitesimal form of the group, and the operator G defined as

$$G = \xi(x, y)\frac{\partial}{\partial x} + \eta(x, y)\frac{\partial}{\partial y} \tag{3.6}$$

and is called the generator of the infinitesimal transformation [5, p 42]. Once (3.6) is known, x^* and y^* can be obtained by solving (3.4)–(3.5).

3.2 Symmetries of ordinary differential equations

An nth order ordinary differential equation [5, p 132–133]

$$E\left(x, y, y', ..., y^{(n)}\right) = 0 \tag{3.7}$$

possesses

$$G = \xi(x, y)\frac{\partial}{\partial x} + \eta(x, y)\frac{\partial}{\partial y} \tag{3.8}$$

as a symmetry if

$$G^{[n]}E\mid_{E=0} = 0, \tag{3.9}$$

where $G^{[n]}$ is the nth extention of G, and is given by [17]

$$G^{[n]} = G + \sum_{i=1}^{n}\left\{\eta^{(i)} - \sum_{j=0}^{i-1}\binom{i}{j}y^{(j+1)}\xi^{(i-j)}\right\}\frac{\partial}{\partial y^{(i)}}. \tag{3.10}$$

The bracketed superscripts in (3.10) refer to total differentiation with respect to the independent variable x. In the case of the first derivative

$$\xi' = \frac{\partial \xi}{\partial x} + y'\frac{\partial \xi}{\partial y}, \tag{3.11}$$

and in the case of the second derivative

$$\xi'' = \frac{\partial^2 \xi}{\partial x^2} + 2y'\frac{\partial^2 \xi}{\partial x \partial y} + y'^2\frac{\partial^2 \xi}{\partial y^2} + y''\frac{\partial \xi}{\partial y}. \tag{3.12}$$

Example 3.2.1. *Consider the following equation (from Kweyama et al [15])*

$$Y'' + \alpha Y' + \frac{2\alpha^2}{9}Y = g_2 Y^3. \tag{3.13}$$

Let

$$G = \xi(X, Y)\frac{\partial}{\partial X} + \eta(X, Y)\frac{\partial}{\partial Y} \tag{3.14}$$

be a symmetry of (3.13). Then the operation of (3.9) with $n = 2$ produces the equation

$$\begin{aligned}\eta\left(\frac{2}{9}\alpha^2 - 3g_2Y^2\right) + \alpha\left(\frac{\partial \eta}{\partial X} + Y'\frac{\partial \eta}{\partial Y} - Y'\frac{\partial \xi}{\partial X} - Y'^2\frac{\partial \xi}{\partial Y}\right) + \frac{\partial^2 \eta}{\partial X^2} + 2Y'\frac{\partial^2 \eta}{\partial X \partial Y}\\ + \left(\frac{\partial \eta}{\partial Y} - 2\frac{\partial \xi}{\partial X} - 3Y'\frac{\partial \xi}{\partial Y}\right)\left(-\alpha Y' - \frac{2\alpha^2}{9}Y + g_2Y^3\right) + Y'^2\frac{\partial^2 \eta}{\partial Y^2} - Y'\frac{\partial^2 \xi}{\partial X^2}\\ - 2Y'^2\frac{\partial^2 \xi}{\partial X \partial Y} - Y'^3\frac{\partial^2 \xi}{\partial Y^2} = 0.\end{aligned} \tag{3.15}$$

Since ξ and η do not depend on derivatives of Y we observe that we can equate coefficients of different powers of Y' in (3.15) to zero. Then (3.15) separates into the system

$$\frac{\partial^2 \xi}{\partial Y^2} = 0, \quad (3.16)$$

$$\frac{\partial^2 \eta}{\partial Y^2} - 2\frac{\partial^2 \xi}{\partial X \partial Y} + 2\alpha \frac{\partial \xi}{\partial Y} = 0, \quad (3.17)$$

$$\alpha \frac{\partial \xi}{\partial X} + 2\frac{\partial^2 \eta}{\partial X \partial Y} - \frac{\partial^2 \xi}{\partial X^2} + \frac{6\alpha^2}{9} Y \frac{\partial \xi}{\partial Y} - 3g_2 Y^3 \frac{\partial \xi}{\partial Y} = 0, \quad (3.18)$$

$$\eta\left(\frac{2}{9}\alpha^2 - 3g_2 Y^2\right) + \alpha \frac{\partial \eta}{\partial X} + \frac{\partial^2 \eta}{\partial X^2} + \left(g_2 Y^3 - \frac{2\alpha^2}{9} Y\right)\frac{\partial \eta}{\partial Y} - \left(2g_2 Y^3 - \frac{4\alpha^2}{9} Y\right)\frac{\partial \xi}{\partial X} = 0. \quad (3.19)$$

We solve (3.16) to obtain

$$\xi = aY + b, \quad (3.20)$$

with $a = a(X)$, $b = b(X)$. Substituting ξ into (3.17) yields

$$\frac{\partial^2 \eta}{\partial Y^2} - 2a' + 2\alpha a = 0, \quad (3.21)$$

and solving we obtain

$$\eta = (a' - \alpha a)\, Y^2 + cY + d, \quad (3.22)$$

where $c = c(X)$ and $d = d(X)$. Now substituting ξ and η in (3.18) and separating using powers of Y we obtain the equations

$$a = 0 \quad (3.23)$$

$$\alpha b' - b'' + 2c' = 0. \quad (3.24)$$

Taking into account $a = 0$ in ξ and η, then the substitution in (3.19) yields to the equations

$$d = 0 \quad (3.25)$$

$$-c = b' \quad (3.26)$$

$$\alpha c' + c'' + \frac{4}{9}\alpha^2 b' = 0. \quad (3.27)$$

Thus (3.24), (3.26) and (3.27) lead to the solutions

$$b = k_0 e^{(\alpha/3)X} + k_1, \quad (3.28)$$

$$c = -\frac{\alpha}{3} k_0 e^{(\alpha/3)X}, \quad (3.29)$$

where k_0 and k_1 are constants. Therefore

$$\xi(X,Y) = k_0 e^{(\alpha/3)X} + k_1 \tag{3.30}$$

$$\eta(X,Y) = -\frac{\alpha}{3} k_0 Y e^{(\alpha/3)X} \tag{3.31}$$

which gives the two symmetries of (3.13)

$$G_1 = \frac{\partial}{\partial X} \tag{3.32}$$

and

$$G_2 = e^{(\alpha/3)X}\frac{\partial}{\partial X} - \frac{\alpha}{3} e^{(\alpha/3)X} Y \frac{\partial}{\partial Y}. \tag{3.33}$$

Since (3.13) is a second order ordinary differential equation, the existence of two Lie point symmetries guarantees its reduction to quadratures as we demonstrated in §3.4. ■

3.3 Lie Algebras

As stated in Chapter 1 (and discussed in detail in §3.4), Lie symmetries can be used to reduce the order of an equation. So it is natural to expect that, given two symmetries of a second order ordinary differential equation, the order could be reduce twice, which means we have integrated the system [17]. We will use Lie algebras to determine the route of reduction.

Definition 3.3.1. *A Lie algebra is a vector space $\mathcal{L}$ together with a bilinear operator [20]*

$$[\cdot,\cdot] : \mathcal{L} \times \mathcal{L} \longrightarrow \mathcal{L},$$

called the Lie bracket for $\mathcal{L}$, satisfying the axioms

i) Bilinearity

$$[cv + c'v', w] = c\,[v,w] + c'[v',w], \quad [v, cw + c'w'] = c[v,w] + c'[v,w'],$$

ii) Skew-symmetry

$$[v,w] = -[w,v],$$

and

iii) Jacobi identity

$$[u,[v,w]]+[v,[w,u]]+[w,[u,v]]=0,$$

for all vectors u, v, v′, w, w′ in the Lie algebra $\mathcal{L}$, and constants c, c′ in $\mathbb{R}$. ■

The Lie bracket is defined as follows [20]

$$[v,w]=vw-wv. \tag{3.34}$$

If a differential equation admits the operators X and Y as symmetry, it also admits their Lie bracket [11]. It may be proved that, if the Lie bracket relation between two symmetries is

$$[X,Y]=\lambda X \tag{3.35}$$

($\lambda=0$ or a constant), then reduction via X will result in $Y^{[1]}$ being a symmetry of the reduced equation [20, p 149].

Example 3.3.2. *From (3.32)–(3.33),*

$$[G_1,G_2]=\frac{\alpha}{3}G_2. \tag{3.36}$$

Thus we use G_2 to reduce (3.13) to order one, and then use G_1 to get the solutions (of the reduced equation). ■

3.4 Reduction of order

Let us consider the second order ordinary differential equation

$$F\left(x,y,y',y''\right)=y''-f\left(x,y,y'\right)=0 \tag{3.37}$$

which admits

$$G=\xi(x,y)\frac{\partial}{\partial x}+\eta(x,y)\frac{\partial}{\partial y} \tag{3.38}$$

as symmetry. Then the second extension of G, $G^{[2]}$, applied to (3.37) when (3.37) is satisfied yields

$$\xi(x,y)\frac{\partial f}{\partial x}+\eta(x,y)\frac{\partial f}{\partial y}+(\eta'-y'\xi')\frac{\partial f}{\partial y'}=\eta''-2\xi' f(x,y,y')-y'\xi''. \tag{3.39}$$

The characteristic equations associated with the PDE (3.39) is

$$\frac{dx}{\xi(x,y)}=\frac{dy}{\eta(x,y)}=\frac{dy'}{\eta'-y'\xi'}. \tag{3.40}$$

The solution of the first equation in (3.40) gives the invariant $u(x,y)$ while the solution of the remaining equation gives the differential invariant $v(x,y,y')$. Inductively it has been shown that, in terms of differential invariants $u(x,y)$ and $v(x,y,y')$, equation (3.37) can be reduced to the first order ordinary differential equation [5, p 125-126]

$$\frac{dv}{du}=H\left(u,v,\frac{dv}{du}\right), \tag{3.41}$$

where H is a function of u, v, dv/du.

Example 3.4.1. *Recall that (3.13) admits the two symmetries (3.32) and (3.33) with Lie bracket (3.36). As result we use G_2 to reduce the order of (3.13). The first prolongation of G_2 is*

$$G_2^{[1]}=e^{(\alpha/3)X}\frac{\partial}{\partial X}-\frac{\alpha}{3}e^{(\alpha/3)X}Y\frac{\partial}{\partial Y}-e^{(\alpha/3)X}\left(\frac{\alpha^2}{9}Y+\frac{2\alpha}{3}Y'\right)\frac{\partial}{\partial Y'}, \tag{3.42}$$

and the characteristic equations are

$$-\frac{\alpha dX}{3}=\frac{dY}{Y}=\frac{dY'}{\frac{\alpha}{3}Y+2Y'}. \tag{3.43}$$

Thus we have two invariants u and v defined as

$$u = Ye^{(\alpha/3)X} \tag{3.44}$$

$$v = \frac{Y'+\frac{\alpha}{3}Y}{Y^2}. \tag{3.45}$$

Using the fact that

$$\frac{dv}{du}=\frac{\frac{dv}{dX}}{\frac{du}{dX}}=\frac{\left(Y''+\frac{\alpha}{3}Y'\right)Y-2Y'\left(Y'+\frac{\alpha}{3}Y\right)}{Y^3\left(Y'+\frac{\alpha}{3}Y\right)e^{(\alpha/3)X}} \tag{3.46}$$

and taking (3.13) into account we obtain

$$\frac{dv}{du} = \frac{\left(-\alpha Y' - \frac{2\alpha^2}{9}Y + g_2Y^3 + \frac{\alpha}{3}Y'\right)Y - 2Y'\left(Y' + \frac{\alpha}{3}Y\right)}{Y^3\left(Y' + \frac{\alpha}{3}Y\right)e^{(\alpha/3)X}} \tag{3.47}$$

$$= \frac{g_2Y^4 - 2\left(Y' + \frac{\alpha}{3}Y\right)^2}{Y^3\left(Y' + \frac{\alpha}{3}Y\right)e^{(\alpha/3)X}}. \tag{3.48}$$

Now taking (3.44)–(3.45) into account we obtain the differential equation

$$\frac{dv}{du} = \frac{g_2}{uv} - \frac{2v}{u}, \tag{3.49}$$

which admits as solutions

$$v = \pm\sqrt{\frac{1}{2}g_2 + ku^{-4}}, \tag{3.50}$$

with k a constant. Substituting u and v in (3.50) from (3.44)–(3.45), we obtain

$$Y'^2 + \frac{\alpha^2}{9}Y^2 + \frac{2\alpha}{3}YY' - \frac{1}{2}g_2Y^4 = ke^{-(4\alpha/3)X}. \tag{3.51}$$

If we set

$$\mathcal{X} = -\frac{3}{\alpha}e^{-(\alpha/3)X} \tag{3.52}$$

$$\mathcal{Y} = e^{(\alpha/3)X}Y, \tag{3.53}$$

then we can rewrite (3.51) as

$$\left(\frac{d\mathcal{Y}}{d\mathcal{X}}\right)^2 - \frac{1}{2}g_2\mathcal{Y}^4 = k \tag{3.54}$$

which can be reduced to the quadrature

$$\mathcal{X} - \mathcal{X}_0 = \int \frac{d\mathcal{Y}}{\sqrt{\frac{1}{2}g_2\mathcal{Y}^4 + k}} \tag{3.55}$$

where $\mathcal{X}_0$ is a constant.

Now we consider G_1. The first prolongation of G_1 given by

$$G_1^{[1]} = \frac{\partial}{\partial X}$$

yields the characteristic equations

$$\frac{dX}{1} = \frac{dY}{0} = \frac{dY'}{0}. \tag{3.56}$$

Thus we have two invariants $u = Y$ *and* $v = Y'$*, which satisfy the differential equation*

$$\frac{dv}{du} = \frac{-\alpha v - \frac{2\alpha^2}{9}u + g_2 u^3}{v}. \tag{3.57}$$

We see that equation (3.57) is not easy to solve, therefore we cannot reduce (3.13) to quadratures using G_1*. Thus the Lie bracket is crucial to making the appropriate choices for the reduction of an equation.* ■

Chapter 4

Application of dynamical systems analysis to a relativistic model

While studying the behaviour of spherically symmetric charged fluids in general relativity, Kweyama *et al* [15] obtained the following underlying ordinary differential equation

$$y'' = f(x)y^2 + g(x)y^3, \tag{4.1}$$

where

$$f(x) = \frac{\tilde{F}(r)}{4r^2}, \tag{4.2}$$

and

$$g(x) = \frac{E^2}{2r^6}. \tag{4.3}$$

In equation (4.1), $x = r^2$, $\tilde{F}$ is an arbitrary function and E is the total charge contained within the sphere of radius r centred around the origin.

Equation (4.1) is the fundamental nonlinear ordinary differential equation which determines the behaviour of self-gravitating charged fluids in general relativity [15]. Kweyama *et al* [15] found that

$$G = a\frac{\partial}{\partial x} + (by + c)\frac{\partial}{\partial y} \tag{4.4}$$

is a symmetry of (4.1), provided the functions $a(x)$, $b(x)$, and $c(x)$ satisfied the following system

of ordinary differential equations:

$$\begin{aligned} a'' &= 2b' && (4.5)\\ b'' &= 2fc && (4.6)\\ c'' &= 0 && (4.7)\\ af' + (2a' + b)f &= -3cg && (4.8)\\ ag' + (2a' + 2b)g &= 0. && (4.9) \end{aligned}$$

This system was reduced to

$$\begin{aligned} 2b &= a' + \alpha && (4.10)\\ c &= c_0 + c_1 x && (4.11)\\ g &= g_2 a^{-3} \exp\left(-\int \frac{\alpha\ dx}{a}\right), && (4.12)\\ f &= a^{-5/2} \exp\left(-\int \frac{\alpha\ dx}{2a}\right)\left[f_2 - 3g_2 \int ca^{-3/2} \exp\left(\int \frac{\alpha\ dx}{a}\right) dx\right], && (4.13) \end{aligned}$$

where α, c_0, c_1, f_2 and g_2 are arbitrary constants. Setting

$$\begin{aligned} X &= \int \frac{dx}{a} && (4.14)\\ Y &= y \exp\left(-\int \frac{b\ dx}{a}\right) - \int \frac{c}{a} \exp\left(-\int \frac{b\ dx}{a}\right) dx, && (4.15) \end{aligned}$$

Kweyama *et al* [15] transformed (4.1) into autonomous form. When $c \neq 0$, a satisfied the nonlinear fourth order equation

$$caa'''' + \left[c\left(\frac{5a'}{2} + \frac{\alpha}{2}\right) - c'a\right] a''' = -12 g_2 c^3 a^{-3} exp\left(-\int \frac{\alpha dx}{a}\right), \qquad (4.16)$$

and (4.1) became

$$Y'' + \alpha Y' + \left(M + \frac{\alpha^2}{4}\right) Y = g_2 Y^3 + f_2 Y^2 + N. \qquad (4.17)$$

When $c = 0$

$$a = a_0 + a_1 x + a_2 x^2, \qquad (4.18)$$

and (4.1) became

$$Y'' + \alpha Y' + \beta Y = g_2 Y^3 + f_2 Y^2, \qquad (4.19)$$

where

$$\beta = -\frac{1}{4}a_1^2 + a_0 a_2 + \frac{1}{4}\alpha^2, \tag{4.20}$$

and M, N, a_0, a_1 and a_2 are constants. The quantities M and N are constants of integration and are given by [15]

$$M = \frac{1}{2}aa'' - \frac{1}{4}a'^2 - 2f_2 I + 3g_2 I^2 \tag{4.21}$$

and

$$N = -a^{-1/2}\exp\left(-\int \frac{\alpha\ dx}{2a}\right)\left(ac' - \frac{1}{2}a'c + \frac{1}{2}\alpha c\right) - \left(\frac{1}{2}aa'' - \frac{1}{4}a'^2 + \frac{\alpha^2}{4}\right) I + f_2 I^2 - 2g_2 I^3, \tag{4.22}$$

where

$$I = \int ca^{-3/2}\exp\left(-\int \frac{\alpha\ dx}{2a}\right) dx. \tag{4.23}$$

The equations (4.17) and (4.19) admit only one symmetry:

$$G_1 = \frac{\partial}{\partial X}. \tag{4.24}$$

Kweyama *et al* [15] investigated the conditions under which equations (4.17) and (4.19) could have an additional symmetry. Our intention is to investigate the impact of all the parameters and of those conditions on the qualitative behaviour of our underlying equations in the phase plane near the equilibrium points. We perform the phase plane analysis in this chapter and relate this to the conditions under which Kweyama *et al* [15] obtained additional symmetries in Chapter 5.

4.1 Non zero c

The first part of our analysis is focused on equation (4.17). If we set

$$U = Y', \tag{4.25}$$

we can rewrite (4.17) as the two-dimensional nonlinear system

$$\begin{aligned} Y' &= U = h(Y,U) \\ U' &= g_2 Y^3 + f_2 Y^2 - \left(M + \frac{\alpha^2}{4}\right) Y - \alpha U + N = k(Y,U). \end{aligned} \tag{4.26}$$

The motion in the phase plane is given by the phase portrait of solutions that comes from system (4.26). The phase portrait is determined by the linear system analysis associated with (4.26) at the equilibrium points. The equilibrium points occur when

$$Y' = 0, \tag{4.27}$$

and

$$U' = 0. \tag{4.28}$$

These imply that

$$U = 0, \tag{4.29}$$

and

$$g_2 Y^3 + f_2 Y^2 - \left(M + \frac{\alpha^2}{4}\right) Y + N = 0. \tag{4.30}$$

Before proceeding with the general analysis, we observe that the function h is odd in U (i.e, $h(Y, -U) = -h(Y, U)$), and when $\alpha = 0$ the function k is even in U (i.e, $k(Y, -U) = k(Y, U)$). Therefore the system is **reversible** (see chapter 2) when $\alpha = 0$. The direction of the vector fields is given by the sign of U in (4.26). Thus Y **increases** when $U > 0$, and **decreases** when $U < 0$.

4.1.1 Neutral dust

Here we take $g_2 = 0$ and $f_2 = 0$ [16]. From (4.12) $g = 0$, therefore there is no charge contained within the sphere ($E = 0$ in (4.3)). The system (4.26) becomes

$$\begin{aligned} Y' &= U \\ U' &= -\left(M + \frac{\alpha^2}{4}\right) Y - \alpha U + N. \end{aligned} \tag{4.31}$$

Since N is constant, the system (4.31) is linear.

1. For $M \neq -\dfrac{\alpha^2}{4}$, $\left(\dfrac{4N}{4M + \alpha^2}, 0\right)$ is the only equilibrium point. At that point, the Jacobian matrix is given by

$$A = \begin{pmatrix} 0 & 1 \\ -\left(M + \dfrac{\alpha^2}{4}\right) & -\alpha \end{pmatrix}. \tag{4.32}$$

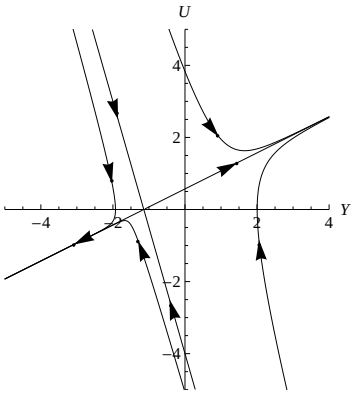

Figure 4.1: Saddle point predicted by the system in the neutral dust when $M < -\frac{\alpha^2}{4}$ ($\alpha = 3$, $M = -4$, $N = 2$).

Thus $\tau = -\alpha$, $\Delta = M + \frac{\alpha^2}{4}$.

(a) If $M < -\frac{\alpha^2}{4}$, then $\Delta < 0$. Therefore, the equilibrium point is a **saddle point**. The behaviour of the solutions is shown in Figure 4.1.

(b) If $-\frac{\alpha^2}{4} < M$, then $\Delta > 0$.
Thus $\tau^2 - 4\Delta = \alpha^2 - 4M - \alpha^2 = -4M$.

i. When $M > 0$, $\tau^2 - 4\Delta < 0$.

A. For $\alpha \neq 0$, we have a **spiral** around the equilibrium point. The spiral is **stable** if $\alpha > 0$, and **unstable** if $\alpha < 0$. The phase portrait of the solutions is shown in Figures 4.2(a)–4.2(b).

B. For $\alpha = 0$, the only equilibrium point $\left(\frac{N}{M}, 0\right)$ is a **centre**, and the direction is given by the sign of U (see the beginning of the section). The phase portrait is shown in Figure 4.2(c).

ii. When $-\frac{\alpha^2}{4} < M < 0$, then $\tau^2 - 4\Delta > 0$, and $\alpha \neq 0$. Therefore the equilibrium point is a **node**. It is a **stable node** if $\alpha > 0$ and an **unstable node** if $\alpha < 0$. The phase portrait of the solutions is given in Figures 4.3(a)–4.3(b).

iii. When $M = 0$, then $\tau^2 - 4\Delta = 0$.

A. If $\alpha = 0$, then $\Delta = 0$. Thus we have a **whole plane** of equilibrium points.

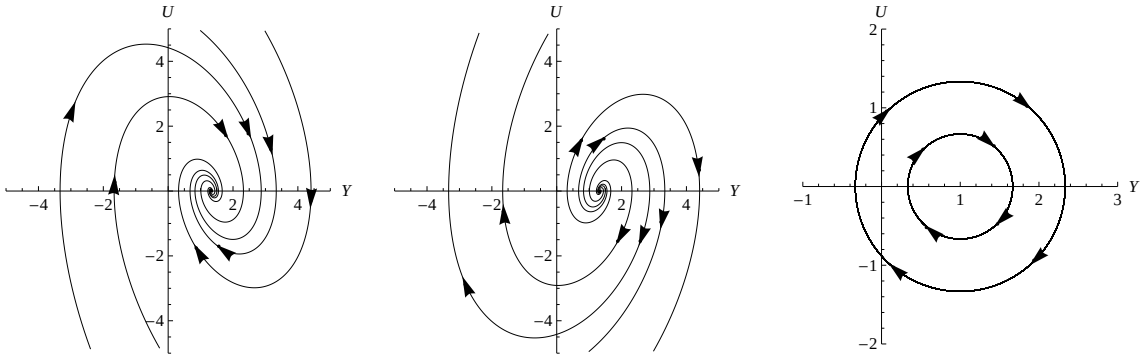

(a) Stable spiral (b) Unstable spiral (c) centre

Figure 4.2: Behaviour of the system in the neutral dust case when $M > 0$. The system predicts a spiral ($\alpha = \pm 1$, $M = 2$, $N = 3$), or a centre ($\alpha = 0$, $M = 1$, $N = 1$).

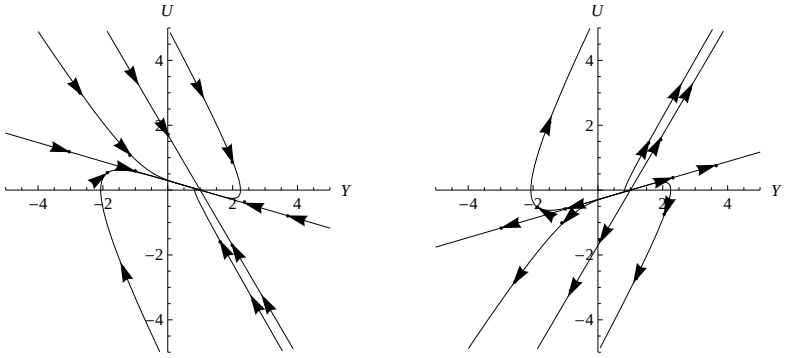

(a) Stable node (b) Unstable node

Figure 4.3: The changes of the behaviour of the system in the neutral dust case when $-\frac{\alpha^2}{4} < M < 0$ predict a node ($\alpha = \pm 2$, $M = -0.5$, $N = 0.5$).

B. If $\alpha \neq 0$, we have a double eigenvalue $\lambda = \frac{\tau}{2} = -\frac{\alpha}{2}$, with one associated eigenvector $V = \left(-\frac{2}{\alpha}, 1\right)$. Thus the equilibrium point is a **degenerate node**. The node is **stable** if $\alpha > 0$, and **unstable** if $\alpha < 0$. The global phase portrait is shown in Figures 4.4(a)–4.4(b).

2. For $M = -\frac{\alpha^2}{4}$, (4.31) becomes

$$\begin{aligned} Y' &= U \\ U' &= -\alpha U + N. \end{aligned} \tag{4.33}$$

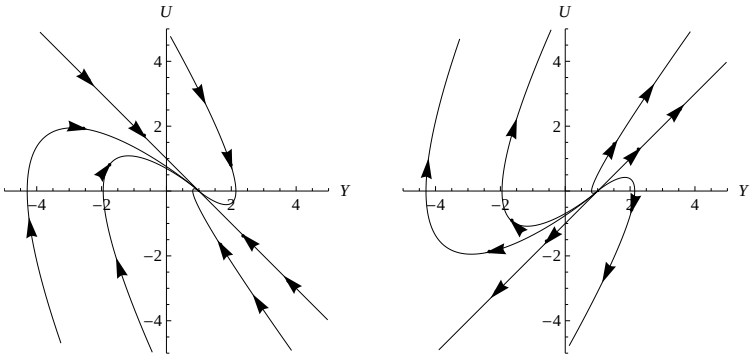

(a) Stable degenerate node (b) Unstable degenerate node

Figure 4.4: Behaviour of the system in the neutral dust case when $M = 0$ and $\alpha \neq 0$. We have a degenerate node ($\alpha = \pm 2$, $M = 0$, $N = 1$).

This system allows an equilibrium point only if $N = 0$. In that case we have the simple solution

$$Y = A + Be^{-\alpha x}, \tag{4.34}$$

when $\alpha \neq 0$, and

$$Y = A + Bx \tag{4.35}$$

when $\alpha = 0$.

4.1.2 Neutral perfect fluid

Here we take $g_2 = 0$ and $f_2 \neq 0$ [16]. Thus there is no charge within the sphere, but we do have matter.

1. When $\alpha = 0$, the system (4.26) becomes

$$\begin{aligned} Y' &= U \\ U' &= f_2 Y^2 - MY + N. \end{aligned} \tag{4.36}$$

There are two equilibrium points

$$(Y_0, 0) = \left(\frac{M + \sqrt{M^2 - 4f_2 N}}{2f_2}, 0 \right), \ (Y_1, 0) = \left(\frac{M - \sqrt{M^2 - 4f_2 N}}{2f_2}, 0 \right), \tag{4.37}$$

provided $M^2 - 4f_2 N \geq 0$.

(a) If $M^2 - 4f_2N = 0$, i.e, $N = \dfrac{M^2}{4f_2}$, then $\left(\dfrac{M}{2f_2}, 0\right)$ is the only equilibrium point, and at that point the Jacobian matrix is given by

$$A = \begin{pmatrix} 0 & 1 \\ 0 & 0 \end{pmatrix}. \tag{4.38}$$

Thus $\tau = 0$ and $\Delta = 0$. We are in a borderline case as discussed in chapter 2 (Table 2.1). We cannot extrapolate from the linear case to the fully nonlinear case. However, system (4.36) yields

$$Y'\left(f_2Y^2 - MY + N\right) = UU', \tag{4.39}$$

i.e,

$$f_2Y'Y^2 - MY'Y + NY' = UU'. \tag{4.40}$$

After integration (4.40) becomes

$$\frac{1}{3}f_2Y^3 - \frac{1}{2}MY^2 + NY + K_0 = \frac{1}{2}U^2, \tag{4.41}$$

where K_0 is a constant. The phase portrait is shown in Figure 4.5(b).

(b) If $M^2 - 4f_2N > 0$, we have two equilibrium points $(Y_0, 0)$ and $(Y_1, 0)$ in (4.37).

I. At $(Y_0, 0)$, the Jacobian matrix is

$$A = \begin{pmatrix} 0 & 1 \\ \sqrt{M^2 - 4f_2N} & 0 \end{pmatrix}. \tag{4.42}$$

Thus $\tau = 0$ and $\Delta = -\sqrt{M^2 - 4f_2N} < 0$. Therefore we have a **saddle point**.

II. At $(Y_1, 0)$, as Jacobian matrix we have

$$A = \begin{pmatrix} 0 & 1 \\ -\sqrt{M^2 - 4f_2N} & 0 \end{pmatrix}. \tag{4.43}$$

Thus $\tau = 0$ and $\Delta = \sqrt{M^2 - 4f_2N} > 0$. Therefore the point is a **linear centre**. Since the system is reversible, then the equilibrium point is a **nonlinear centre**. The phase portrait is shown in Figure 4.5(a).

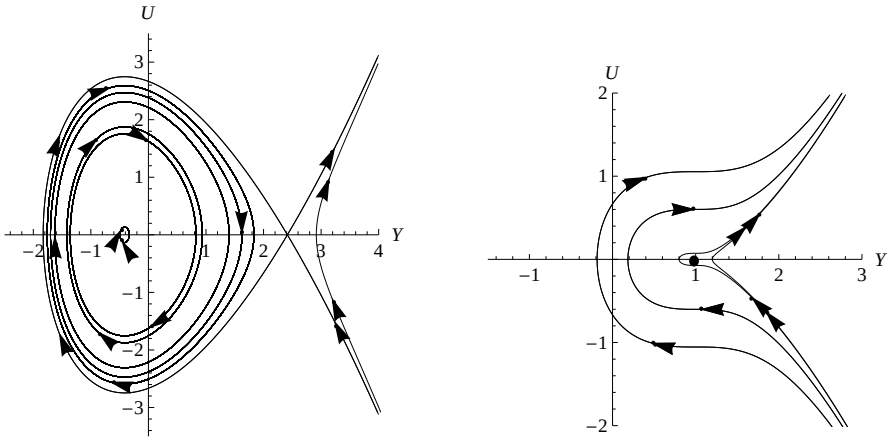

(a) Case $M^2 - 4f_2N > 0$ (b) Case $M^2 - 4f_2N = 0$

Figure 4.5: Behaviour of the system in the neutral perfect fluid case where $\alpha = 0$ ($f_2 = 1$, $M = 2$, and $N = -1$ for (a) and $N = 1$ for (b)).

From (4.37) if $f_2 > 0$, the equilibrium points exist when $N < \dfrac{M^2}{4f_2}$, and then fuse together when $N = \dfrac{M^2}{4f_2}$, and disappear when $N > \dfrac{M^2}{4f_2}$. There has been a **saddle-node bifurcation**.

Similarly, if $f_2 < 0$, the equilibrium points exist when $N > \dfrac{M^2}{4f_2}$, and then fuse when $N = \dfrac{M^2}{4f_2}$, and are destroyed when $N < \dfrac{M^2}{4f_2}$. Therefore we still have a **saddle-node bifurcation**, specifically a **blue sky bifurcation**. Here, N is the **bifurcation parameter** (and not f_2 as it cannot be zero). We can visualize the bifurcation diagram as shown in Figure 4.6.

2. If $\alpha \neq 0$, we have the following equilibrium points

$$(Y_0, 0) = \left(\frac{4M + \alpha^2 + \sqrt{16M^2 - 64f_2N + 8M\alpha^2 + \alpha^4}}{8f_2}, 0 \right) \tag{4.44}$$

and

$$(Y_1, 0) = \left(\frac{4M + \alpha^2 - \sqrt{16M^2 - 64f_2N + 8M\alpha^2 + \alpha^4}}{8f_2}, 0 \right), \tag{4.45}$$

provided $16M^2 - 64f_2N + 8M\alpha^2 + \alpha^4 \geq 0$.

(a) If we assume that $16M^2 - 64f_2N + 8M\alpha^2 + \alpha^4 > 0$, then:

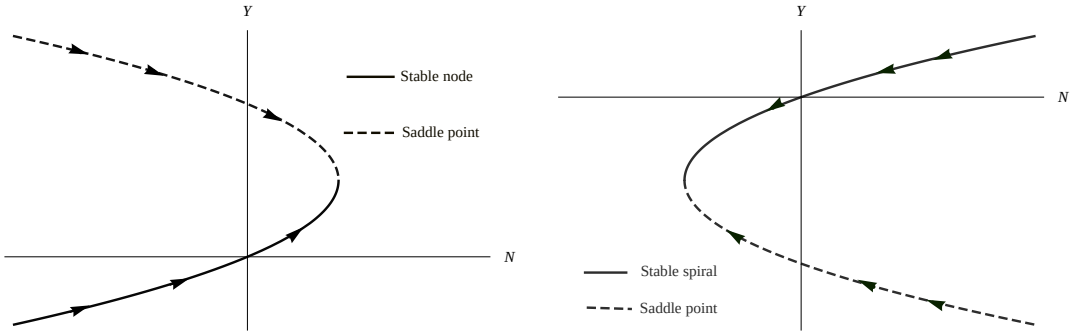

(a) $f_2 > 0$: saddle-node bifurcation (b) $f_2 < 0$: blue sky bifurcation

Figure 4.6: Bifurcation diagram $Y = f(N)$ ($f_2 = \pm 1$ and $M = 2$).

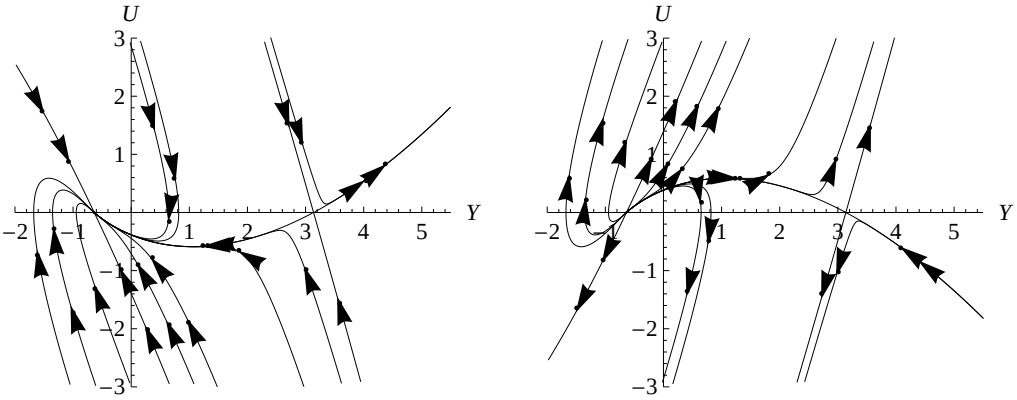

(a) Saddle point, stable node (b) Saddle point, unstable node

Figure 4.7: Node and saddle point predicted by the system when $16M^2 - 64f_2N + 8M\alpha^2 + \alpha^4 > 0$ and $\alpha^2 > \sqrt{16M^2 - 64f_2N + 8M\alpha^2 + \alpha^4}$ ($f_2 = 0.5$, $M = -1$, $N = -1$, $\alpha = \pm 3$).

I. At $(Y_0, 0)$, the Jacobian matrix is given by

$$A = \begin{pmatrix} 0 & 1 \\ \frac{1}{4}\sqrt{16M^2 - 64f_2N + 8M\alpha^2 + \alpha^4} & -\alpha \end{pmatrix}. \tag{4.46}$$

Thus $\tau = -\alpha$ and $\Delta = -\frac{1}{4}\sqrt{16M^2 - 64f_2N + 8M\alpha^2 + \alpha^4} < 0$. Therefore the point is a **saddle point**.

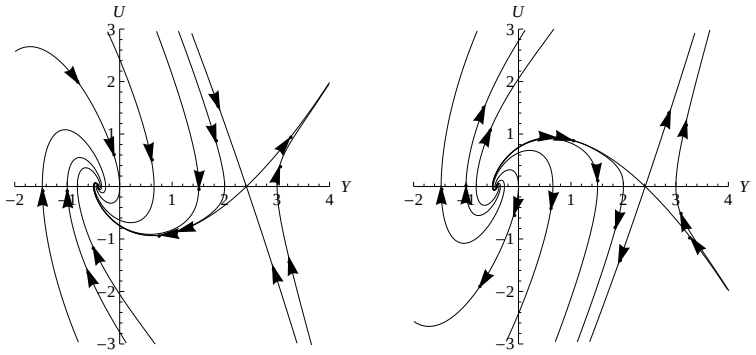

(a) Saddle point, stable spiral (b) Saddle point, unstable spiral

Figure 4.8: Spiral and saddle point predicted by the system when $16M^2-64f_2N+8M\alpha^2+\alpha^4 > 0$ and $\alpha^2 < \sqrt{16M^2-64f_2N+8M\alpha^2+\alpha^4}$ ($f_2 = 1$, $M = 1$, $N = -1$, $\alpha = \pm 2$).

II. At $(Y_1, 0)$, the Jacobian matrix given by

$$A = \begin{pmatrix} 0 & 1 \\ -\frac{1}{4}\sqrt{16M^2-64f_2N+8M\alpha^2+\alpha^4} & -\alpha \end{pmatrix}, \tag{4.47}$$

yields $\tau = -\alpha$ and $\Delta = \frac{1}{4}\sqrt{16M^2-64f_2N+8M\alpha^2+\alpha^4} > 0$.

i) If $\tau^2 - 4\Delta = \alpha^2 - \sqrt{16M^2-64f_2N+8M\alpha^2+\alpha^4} > 0$, then the equilibrium point is a **node**. The node is **stable** when $\alpha > 0$, and **unstable** when $\alpha < 0$. The behaviour is shown in Figures 4.7(a)–4.7(b).

ii) If $\tau^2 - 4\Delta = \alpha^2 - \sqrt{16M^2-64f_2N+8M\alpha^2+\alpha^4} < 0$, we have a **spiral**. It is a **stable** spiral for $\alpha > 0$, and **unstable** spiral for $\alpha < 0$ (as shown in Figures 4.8(a)–4.8(b)).

(b) If we assume that $16M^2 - 64f_2N + 8M\alpha^2 + \alpha^4 = 0$, $\left(\frac{4M+\alpha^2}{8f_2}, 0\right)$ is the only equilibrium point, and at that point the Jacobian matrix is given by

$$A = \begin{pmatrix} 0 & 1 \\ 0 & -\alpha \end{pmatrix}. \tag{4.48}$$

Thus $\tau = -\alpha$ and $\Delta = 0$. We are in a borderline case. Since our system is nonlinear and difficult to solve analytically, we have only plotted the full system numerically

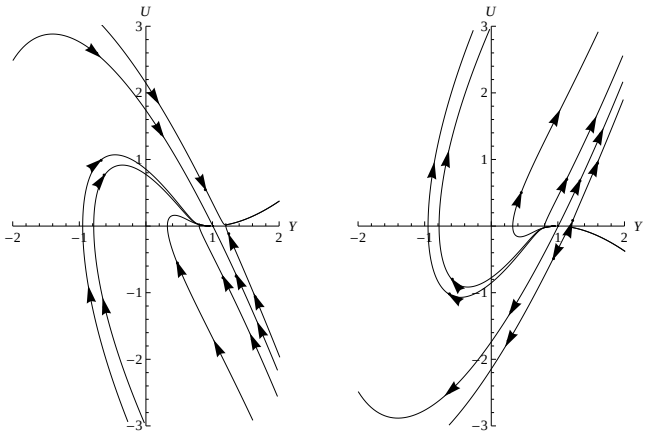

(a) $\alpha > 0$ (b) $\alpha < 0$

Figure 4.9: Behaviour of the system when $16M^2 - 64f_2N + 8M\alpha^2 + \alpha^4 = 0$ (the linear analysis classified as a borderline case). We have plotted using $f_2 = 1$, $M = 1$, $N = 1$, $\alpha = \pm 2$.

with specific values of parameters just to show the behaviour in the phase space, as shown in Figures 4.9(a)–4.9(b) (we used the package Dynpac [7]).

From (4.44) and (4.45), when $\alpha > 0$ we have a bifurcation (because when $\alpha < 0$ all the equilibrium points are unstable, and there is no change of stability). Thus for $f_2 > 0$, the two equilibrium points exist when $N < \dfrac{16M^2 + 8M\alpha^2 + \alpha^4}{64f_2}$, then fuse when $N = \dfrac{16M^2 + 8M\alpha^2 + \alpha^4}{64f_2}$, and disappear when $N > \dfrac{16M^2 + 8M\alpha^2 + \alpha^4}{64f_2}$. A **saddle-node bifurcation** occurred.

Likewise, for $f_2 < 0$ the opposite happens. We have a **blue sky bifurcation**, with N as the **bifurcation parameter**. The bifurcation diagram is shown in Figure 4.10.

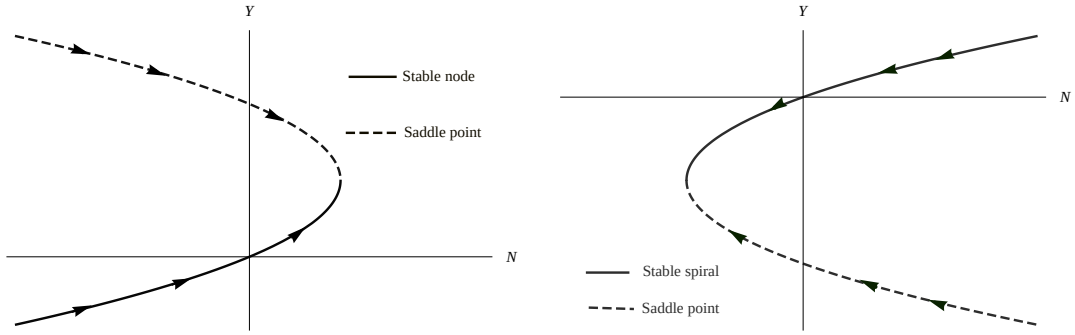

(a) $f_2 > 0$: saddle-node bifurcation (b) $f_2 < 0$: blue sky bifurcation

Figure 4.10: Bifurcation diagram $Y = f(N)$ ($f_2 = 0.5$, $M = -1$, $\alpha = 3$ for figure (a), and $M = 1$, $f_2 = -1$ and $\alpha = 2$ for figure (b)).

4.1.3 Charged fluid

We now insist on $g_2 \neq 0$. Thus $E \neq 0$ and the matter is charged. The equation (4.30) admits as solutions

$$Y_0 = -\frac{f_2}{3g_2} + \frac{16f_2^2 + 48g_2M + 12g_2\alpha^2}{6\sqrt[3]{4}g_2\delta} + \frac{\delta}{12\sqrt[3]{2}g_2}, \tag{4.49}$$

$$Y_1 = -\frac{f_2}{3g_2} - \frac{(1+i\sqrt{3})(16f_2^2 + 48g_2M + 12g_2\alpha^2)}{12\sqrt[3]{4}g_2\delta} - \frac{(1-i\sqrt{3})\delta}{24\sqrt[3]{2}g_2}, \tag{4.50}$$

$$Y_2 = -\frac{f_2}{3g_2} - \frac{(1-i\sqrt{3})(16f_2^2 + 48g_2M + 12g_2\alpha^2)}{12\sqrt[3]{4}g_2\delta} - \frac{(1+i\sqrt{3})\delta}{24\sqrt[3]{2}g_2}, \tag{4.51}$$

provided $16f_2^2 + 48g_2M + 12g_2\alpha^2 \neq 0$ [13, 14, 26], with

$$\delta = \left(-128f_2^3 - 576f_2g_2M - 1728g_2^2N - 144f_2g_2\alpha^2 + \delta_1\right)^{\frac{1}{3}}, \tag{4.52}$$

and

$$\delta_1 = \sqrt{(-128f_2^3 - 576f_2g_2M - 1728g_2^2N - 144f_2g_2\alpha^2)^2 - 4(16f_2^2 + 48g_2M + 12g_2\alpha^2)^3}. \tag{4.53}$$

We use this condition because δ could be zero. It is clear that any of these points Y_0, Y_1, Y_2 could be zero.

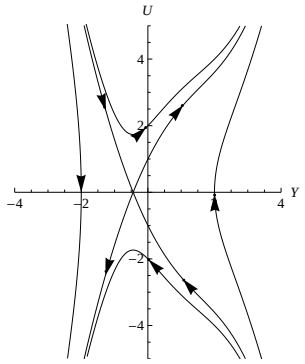

Figure 4.11: Saddle point predicted when $16f_2^2 + 48g_2M + 12g_2\alpha^2 = 0$ in the charged fluid, provided $f_2^3 - 27g_2^2N \neq 0$ and $g_2 > 0$ ($f_2 = -3$, $g_2 = 1$, $M = -3$, $N = 2$, $\alpha = 0$).

1. If $16f_2^2 + 48g_2M + 12g_2\alpha^2 = 0$, i.e, $M = \dfrac{-4f_2^2 - 3g_2\alpha^2}{12g_2}$, equation (4.30) admits

$$Y_{00} = -\frac{f_2}{3g_2} + \frac{(f_2^3g_2^3 - 27g_2^5N)^{\frac{1}{3}}}{3g_2^2}, \tag{4.54}$$

$$Y_{11} = -\frac{f_2}{3g_2} - \frac{(1 - i\sqrt{3})\,(f_2^3g_2^3 - 27g_2^5N)^{\frac{1}{3}}}{6g_2^2}, \tag{4.55}$$

$$Y_{22} = -\frac{f_2}{3g_2} - \frac{(1 + i\sqrt{3})\,(f_2^3g_2^3 - 27g_2^5N)^{\frac{1}{3}}}{6g_2^2} \tag{4.56}$$

as solutions. Since we are interested in real values, the only possible equilibrium point is $(Y_{00}, 0)$. At that point, the Jacobian matrix given by

$$A = \begin{pmatrix} 0 & 1 \\ \dfrac{(f_2^3g_2^3 - 27g_2^5N)^{\frac{2}{3}}}{3g_2^3} & -\alpha \end{pmatrix}, \tag{4.57}$$

yields $\tau = -\alpha$ and $\Delta = -\dfrac{(f_2^3g_2^3 - 27g_2^5N)^{\frac{2}{3}}}{3g_2^3}$.

   (a) If $f_2^3 - 27g_2^2N \neq 0$ and $g_2 > 0$, then $\Delta < 0$. Therefore $(Y_{00}, 0)$ is a **saddle point**. The behaviour is shown in Figure 4.11.

   (b) If $f_2^3 - 27g_2^2N \neq 0$ and $g_2 < 0$, then $\Delta > 0$. If we assume that $\alpha = 0$, $(Y_{00}, 0)$ is a **nonlinear centre** (since the system is reversible). The behaviour is shown in Figure 4.12.

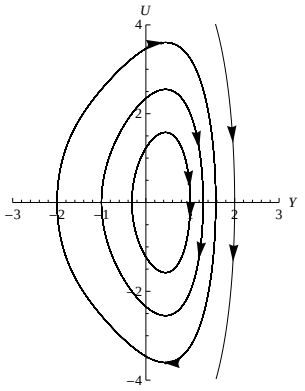

Figure 4.12: Centre predicted when $16f_2^2 + 48g_2M + 12g_2\alpha^2 = 0$ in the charged fluid, provided $f_2^3 - 27g_2^2N \neq 0$, $g_2 < 0$ and $\alpha = 0$ ($f_2 = -3$, $g_2 = -1$, $M = 3$, $N = 2$).

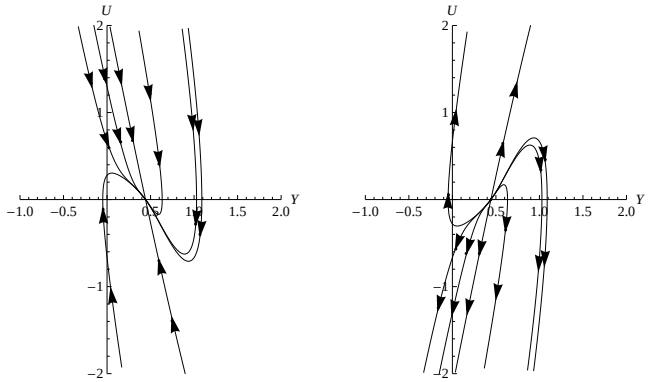

(a) Stable node (b) Unstable node

Figure 4.13: Nodes predicted when $16f_2^2 + 48g_2M + 12g_2\alpha^2 = 0$ in the charged fluid ($f_2 = -3$, $g_2 = -1$, $M = -6$, $N = 2$, $\alpha = \pm 6$).

However, if $\alpha \neq 0$, the point is **stable** when $\alpha > 0$, and **unstable** when $\alpha < 0$. Note that

$$\tau^2 - 4\Delta = \alpha^2 + \frac{4\left(f_2^3 g_2^3 - 27g_2^5 N\right)^{\frac{2}{3}}}{3g_2^3}. \tag{4.58}$$

i. If $\tau^2 - 4\Delta > 0$, the point is a **node** (see Figures 4.13(a)–4.13(b)).

ii. If $\tau^2 - 4\Delta < 0$, we have a **spiral**, as shown in Figures 4.14(a)–4.14(b).

iii. If $\tau^2 - 4\Delta = 0$, the linear equilibrium point is a **degenerate node**. This is a

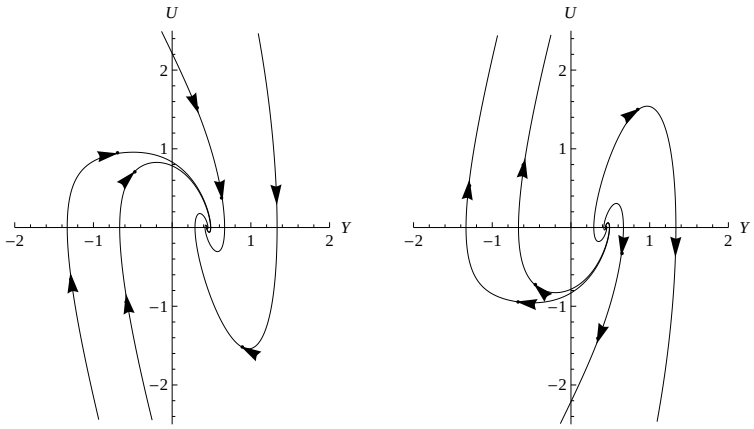

(a) Stable spiral (b) Unstable spiral

Figure 4.14: Spirals predicted when $16f_2^2 + 48g_2M + 12g_2\alpha^2 = 0$ in the charged fluid ($f_2 = -3$, $g_2 = -1$, $M = \dfrac{3}{4}$, $N = 2$, $\alpha = \pm 3$).

borderline case, similarly we have numerically solved the full system to see the effect on the behaviour, as shown in Figures 4.15(a)–4.15(b).

(c) If $f_2^3 - 27g_2^2N = 0$, then $\Delta = 0$. We are also in a borderline case. The behaviour for different values of parameters is shown in Figures 4.16(a)–4.16(b).

2. If $16f_2^2+48g_2M+12g_2\alpha^2 < 0$, then δ in (4.52) is real. Therefore Y_0 in (4.49) is real, whereas Y_1 and Y_2 in (4.50) and (4.51) are still complex. Thus $(Y_0, 0)$ is the only equilibrium point. At that point, the Jacobian matrix is given by

$$A = \begin{pmatrix} 0 & 1 \\ 3g_2Y_0^2 + 2f_2Y_0 - \left(M + \dfrac{\alpha^2}{4}\right) & -\alpha \end{pmatrix}. \tag{4.59}$$

Therefore $\tau = -\alpha$ and $\Delta = -3g_2Y_0^2 - 2f_2Y_0 + \left(M + \dfrac{\alpha^2}{4}\right)$ (which cannot be zero).

(a) If $\Delta < 0$, $(Y_0, 0)$ is a **saddle point** (as shown in Figure 4.17).

(b) If $\Delta > 0$, for $\alpha = 0$, the equilibrium point is a **nonlinear centre** (Figure 4.18). However, for $\alpha \neq 0$, $\tau^2 - 4\Delta = 12g_2Y_0^2 + 8f_2Y_0 - 4M$. The equilibrium point is **stable** when $\alpha > 0$, and **unstable** when $\alpha < 0$.

- If $\tau^2 - 4\Delta > 0$, then $(Y_0, 0)$ is a **node** (Figures 4.19(a)–4.19(b)).

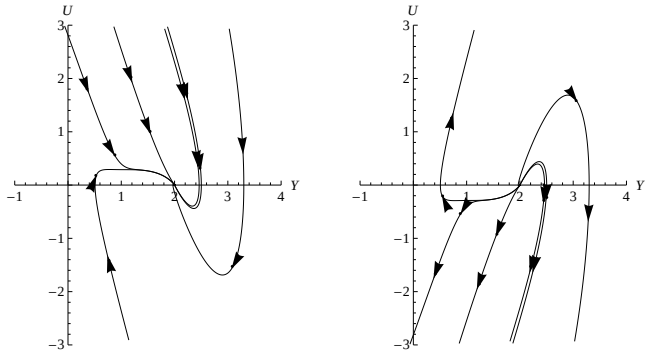

(a) Stable node (b) Unstable node

Figure 4.15: Nodes predicted when $16f_2^2 + 48g_2M + 12g_2\alpha^2 = 0$ in the charged fluid ($f_2 = 3$, $g_2 = -1$, $M = 0$, $N = 2$, $\alpha = \pm 2\sqrt{3}$).

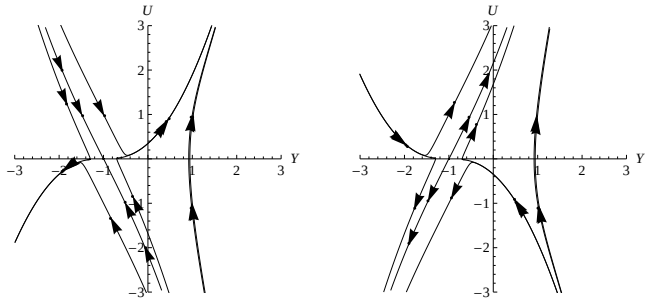

(a) $\alpha > 0$ (b) $\alpha < 0$

Figure 4.16: Behaviour of the system when $\Delta = 0$ and $16f_2^2 + 48g_2M + 12g_2\alpha^2 = 0$ in the charged fluid ($f_2 = 3$, $g_2 = 1$, $M = -4$, $N = 1$, $\alpha = \pm 2$).

- If $\tau^2 - 4\Delta < 0$, then $(Y_0, 0)$ is a **spiral** (Figures 4.20(a)–4.20(b)).
- If $\tau^2 - 4\Delta = 0$, the linear point is a **degenerate node**. As before, we solve the full nonlinear system numerically to determine its behaviour (see Figure 4.21).

3. If $16f_2^2 + 48g_2M + 12g_2\alpha^2 > 0$, Y_0, Y_1 and Y_2 in (4.49), (4.50), (4.51) can be real or complex, but we are only interested in real values. It is difficult to transform them into the form $A + iB$ (where A and B are real), because δ in (4.52) can also be complex, and not easily transformable in this form.

   We will restrict ourselves to the constraint obtained in [15], with $g_2 > 0$. It was shown

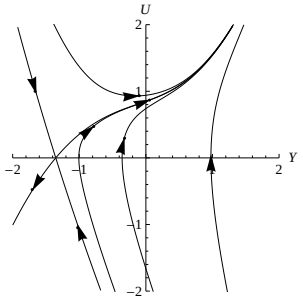

Figure 4.17: Saddle point predicted when $16f_2^2 + 48g_2M + 12g_2\alpha^2 < 0$ in the charged fluid ($f_2 = 1$, $g_2 = 1$, $M = -2$, $N = 2$, $\alpha = 2$).

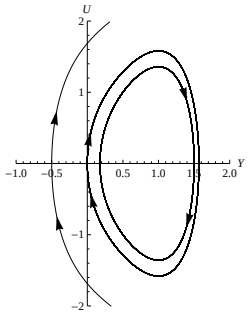

Figure 4.18: Centre predicted when $16f_2^2 + 48g_2M < 0$ and $\alpha = 0$ in the charged fluid ($f_2 = 3$, $g_2 = -3$, $M = 2$, $N = 2$).

that

$$M = -\frac{f_2^2}{3g_2} - \frac{\alpha^2}{36}, \quad N = \frac{f_2^3}{27g_2^2} - \frac{2\alpha^2 f_2}{27g_2} \tag{4.60}$$

led to the additional symmetry

$$G_2 = e^{(\alpha/3)X}\frac{\partial}{\partial X} - e^{(\alpha/3)X}\left(\frac{\alpha}{3}Y + \frac{\alpha f_2}{9g_2}\right)\frac{\partial}{\partial Y}. \tag{4.61}$$

By substituting M and N in (4.49), (4.50) and (4.51) by (4.60), we have three equilibrium points

$$(Y_0, 0) = \left(-\frac{f_2}{3g_2}, 0\right), (Y_1, 0) = \left(-\frac{f_2}{3g_2} - \frac{\sqrt{2}\alpha}{3\sqrt{g_2}}, 0\right), (Y_2, 0) = \left(-\frac{f_2}{3g_2} + \frac{\sqrt{2}\alpha}{3\sqrt{g_2}}\right). \tag{4.62}$$

(a) Assume that $\alpha \neq 0$.

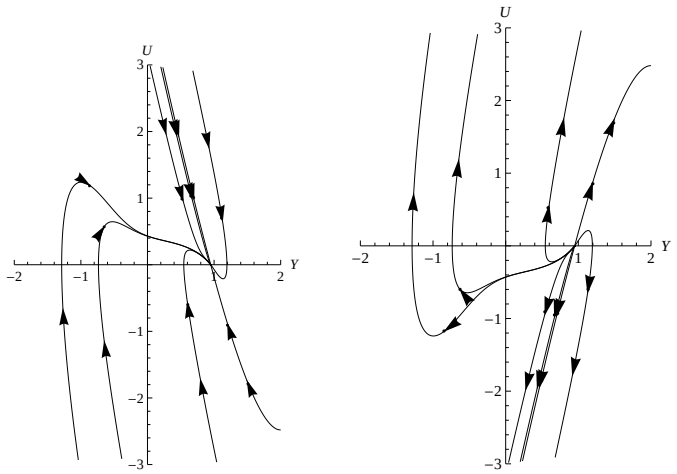

(a) table node (b) unstable node

Figure 4.19: Nodes predicted when $16f_2^2 + 48g_2M + 12g_2\alpha^2 < 0$ in the charged fluid ($f_2 = 1$, $g_2 = -2$, $M = -5$, $N = 2$, $\alpha = \pm 5$).

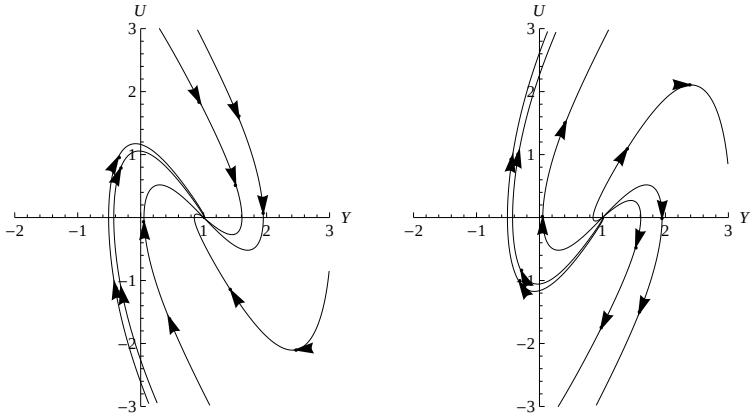

(a) stable spiral (b) unstable spiral

Figure 4.21: Spirals node predicted when $16f_2^2 + 48g_2M + 12g_2\alpha^2 < 0$ by the simulated system (4.26) ($f_2 = 3$, $g_2 = -1$, $M = 3$, $N = 2$, $\alpha = \pm 2$).

I. At $(Y_0, 0)$, the Jacobian matrix given by

$$A = \begin{pmatrix} 0 & 1 \\ -\dfrac{2\alpha^2}{9} & -\alpha \end{pmatrix}, \tag{4.63}$$

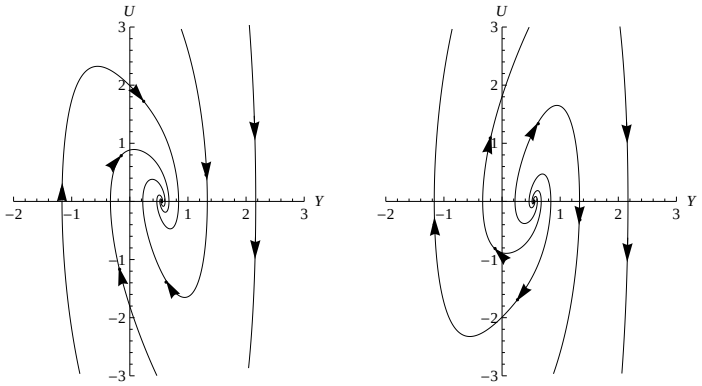

(a) stable spiral (b) unstable spiral

Figure 4.20: Spirals predicted when $16f_2^2 + 48g_2M + 12g_2\alpha^2 < 0$ by (4.26) in the charged fluid ($f_2 = 1$, $g_2 = -4$, $M = 2$, $N = 2$, $\alpha = \pm 2$).

yields

$$\tau = -\alpha,\ \Delta = \frac{2\alpha^2}{9}. \tag{4.64}$$

Since $\Delta > 0$, $\tau^2 - 4\Delta = \alpha^2 - \frac{8\alpha^2}{9} = \frac{\alpha^2}{9} > 0$. Therefore the eigenvalues are real and have the same sign, hence the equilibrium point is a **node**.

- If $\alpha > 0$, then $\tau < 0$. Thus $(Y_0, 0)$ is a **stable node**.
- If $\alpha < 0$, then $\tau > 0$. Thus $(Y_0, 0)$ is an **unstable node**.

II. At $(Y_1, 0)$ and $(Y_2, 0)$, we find as Jacobian matrix

$$A = \begin{pmatrix} 0 & 1 \\ \frac{4\alpha^2}{9} & -\alpha \end{pmatrix}. \tag{4.65}$$

Thus

$$\Delta = -\frac{4\alpha^2}{9}. \tag{4.66}$$

Since $\Delta < 0$, $(Y_1, 0)$ and $(Y_2, 0)$ are **saddle points**. We depict the global phase portrait of the solutions in Figures 4.22(a)–4.22(b).

(b) If $\alpha = 0$, $\left(-\frac{f_2}{3g_2}, 0\right)$ is the only equilibrium point, and at that point

$$\tau = 0,\ \Delta = 0. \tag{4.67}$$

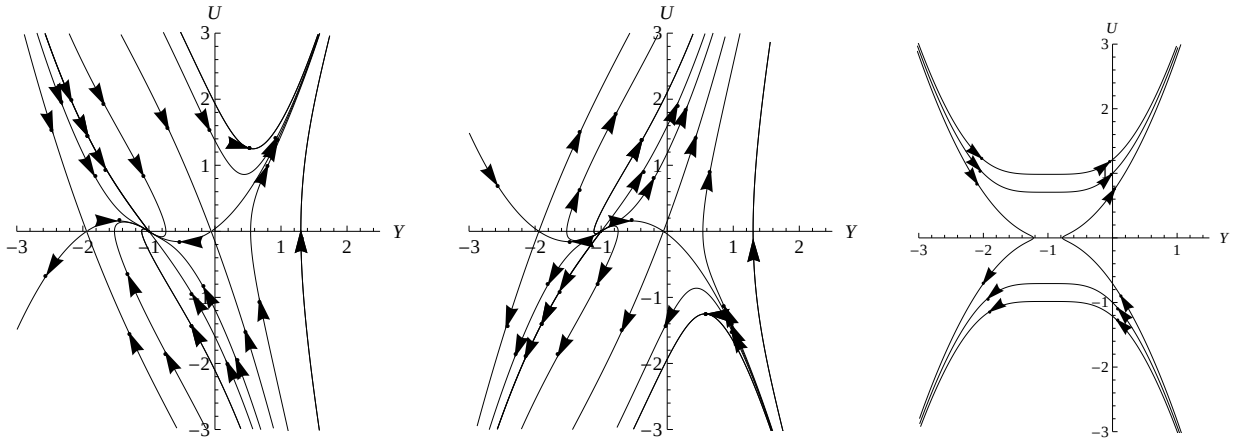

(a) Case $\alpha > 0$ (b) Case $\alpha < 0$ (c) Case $\alpha = 0$

Figure 4.22: Changes of the system in charged fluid when $16f_2^2 + 48g_2M + 12g_2\alpha^2 > 0$, and M and N given by 4.60 ($f_2 = 3$, $g_2 = 1$, $\alpha = \pm 2$ for figures (a) and (b), and with $f_2 = 3$, $g_2 = 1$, $\alpha = 0$ for figures (c)).

This is a borderline case. Here we can show the global behaviour of the full system by reducing (4.26) to the equation

$$UU' = \left(g_2Y^3 + f_2Y^2 - \left(M + \frac{\alpha^2}{4}\right)Y - \alpha U + N\right)Y', \tag{4.68}$$

and then integrate to obtain

$$U^2 = \frac{1}{2}g_2Y^4 + \frac{2}{3}f_3Y^3 - MY^2 + 2NY + 2K_1, \tag{4.69}$$

where K_1 is a constant. The behaviour is obtained by sketching the above implicit function (4.69) as shown in Figure 4.22(c).

4.2 Zero c

The second part of our analysis concerns the nonlinear second order equation (4.19)

$$Y'' + \alpha Y' + \beta Y = g_2Y^3 + f_2Y^2. \tag{4.70}$$

Since $\beta = \gamma + \frac{1}{4}\alpha^2$, with γ an arbitrary constant, this equation is the same as (4.17) with $M = \gamma$ and $N = 0$.

4.2.1 Neutral perfect fluid

Here we take $g_2 = 0$. Whatever the value of f_2 the condition $N = 0$ (according to the previous section) does not affect the existence and the stability of the equilibrium point. Therefore we have the same behaviour of solutions in the phase space. However, there is no bifurcation (since N is constant).

4.2.2 Charged fluid

Now we take $g_2 \neq 0$. Setting

$$U = Y', \tag{4.71}$$

equation (4.70) becomes the two-dimensional nonlinear system

$$\begin{aligned} Y' &= U \\ U' &= g_2 Y^3 + f_2 Y^2 - \beta Y - \alpha U. \end{aligned} \tag{4.72}$$

The equilibrium points are solutions of the system

$$U = 0, \tag{4.73}$$

$$g_2 Y^3 + f_2 Y^2 - \beta Y = 0. \tag{4.74}$$

Equation (4.74) admits three solutions

$$Y_0 = 0, \tag{4.75}$$

$$Y_1 = \frac{-f_2 - \sqrt{f_2^2 + 4g_2\beta}}{2g_2}, \tag{4.76}$$

$$Y_2 = \frac{-f_2 + \sqrt{f_2^2 + 4g_2\beta}}{2g_2}. \tag{4.77}$$

We have four possible cases: $f_2^2 + 4g_2\beta < 0$ and $\beta \neq 0$, $f_2^2 + 4g_2\beta > 0$ and $\beta \neq 0$, $f_2^2 + 4g_2\beta > 0$ and $\beta = 0$, or $f_2^2 + 4g_2\beta = 0$.

When $\alpha = 0$, the system is **reversible**, and the direction of the vector fields is given by the sign of U in (4.72). Thus Y **increases** when $U > 0$, and **decreases** when $U < 0$.

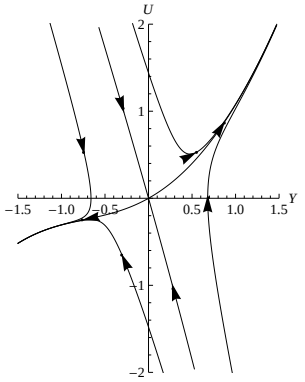

Figure 4.23: Saddle point predicted in charged fluid when $f_2^2 + 4g_2\beta < 0$ and $\beta < 0$.

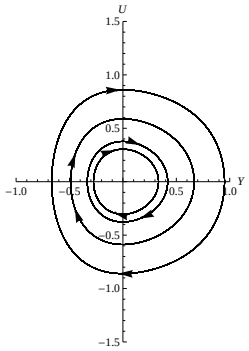

Figure 4.24: Centre at the origin in charged fluid when $f_2^2 + 4g_2\beta < 0$, $\beta > 0$ and $\alpha = 0$.

1. If $f_2^2 + 4g_2\beta < 0$ and $\beta \neq 0$, there is only one equilibrium point, the origin. At the origin, the Jacobian matrix is given by

$$A = \begin{pmatrix} 0 & 1 \\ -\beta & -\alpha \end{pmatrix}. \tag{4.78}$$

Thus

$$\tau = -\alpha,\ \Delta = \beta. \tag{4.79}$$

   (a) If $\beta < 0$, then $\Delta < 0$. Therefore the origin is a **saddle point** (see Figure 4.23).

   (b) If $\beta > 0$, for $\alpha = 0$ the origin is a **nonlinear centre** (since the system is reversible). The phase portrait is shown in Figure 4.24.

   However for $\alpha \neq 0$, note that $\tau^2 - 4\Delta = \alpha^2 - 4\beta$. The point is **stable** when $\alpha > 0$, and **unstable** when $\alpha < 0$.

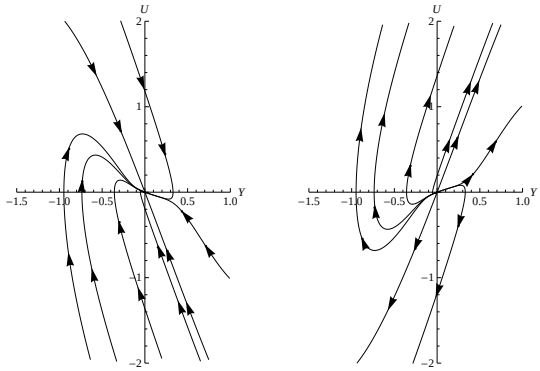

(a) Stable node (b) Unstable node

Figure 4.25: Node at the origin in charged fluid when $f_2^2 + 4g_2\beta < 0$ and $0 < \beta < \dfrac{\alpha^2}{4}$.

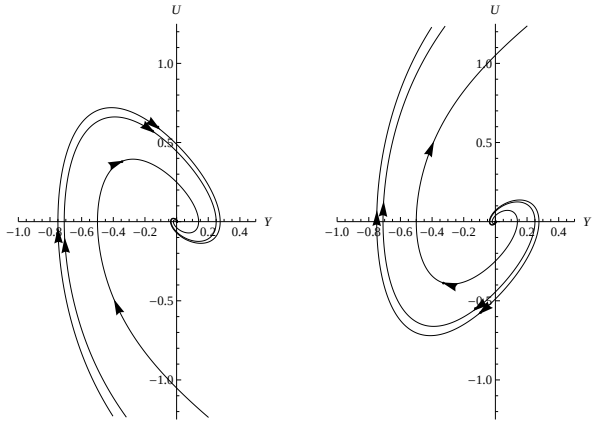

(a) Stable spiral (b) Unstable spiral

Figure 4.26: Spiral at the origin in charged fluid when $f_2^2 + 4g_2\beta < 0$ and $\beta > \dfrac{\alpha^2}{4} > 0$.

- If $0 < \beta < \dfrac{\alpha^2}{4}$, the origin is a **node** (Figures 4.25(a)–4.25(b)).
- If $\beta > \dfrac{\alpha^2}{4}$, we have a **spiral** (Figures 4.26(a)–4.26(b)).
- If $\beta = \dfrac{\alpha^2}{4}$, the origin is a linear **degenerate node**. As in the others cases, the behaviour of the full system (4.19) is obtained by a numerical simulation, as shown in Figures 4.27(a)–4.27(b).

2. If $f_2^2 + 4g_2\beta > 0$ and $\beta \neq 0$, we have two additional equilibrium points $(Y_1, 0)$ and $(Y_2, 0)$

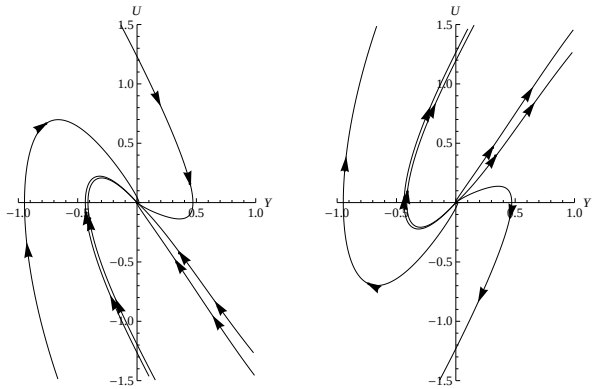

(a) Stable node (b) Unstable node

Figure 4.27: Node at the origin in charged fluid when $f_2^2 + 4g_2\beta < 0$ and $\beta = \dfrac{\alpha^2}{4} > 0$.

given by (4.76) and (4.77).

I. At $(Y_1, 0)$, the Jacobian matrix is

$$A = \begin{pmatrix} 0 & 1 \\ \dfrac{f_2^2 + 4g_2\beta + f_2\sqrt{f_2^2 + 4g_2\beta}}{2g_2} & -\alpha \end{pmatrix}. \tag{4.80}$$

Therefore

$$\tau = -\alpha,\ \Delta = -\frac{f_2^2 + 4g_2\beta + f_2\sqrt{f_2^2 + 4g_2\beta}}{2g_2}. \tag{4.81}$$

In this case $\Delta \neq 0$.

(a) If $\Delta < 0$, then $(Y_1, 0)$ is a **saddle point**.

(b) If $\Delta > 0$, for $\alpha = 0$, $(Y_1, 0)$ is a **centre**.

However, for $\alpha \neq 0$, the point is **stable** when $\alpha > 0$, and **unstable** when $\alpha < 0$. Note that

$$\tau^2 - 4\Delta = \alpha^2 + \frac{2\left(f_2^2 + 4g_2\beta + f_2\sqrt{f_2^2 + 4g_2\beta}\right)}{g_2}. \tag{4.82}$$

i. If $\tau^2 - 4\Delta > 0$, then $(Y_2, 0)$ is a **node**.

ii. If $\tau^2 - 4\Delta < 0$, then we have **spiral node**.

iii. If $\tau^2 - 4\Delta = 0$, then $(Y_1, 0)$ is a linear **degenerate node**. We have solved the system numerically to get the behaviour of the nonlinear analysis.

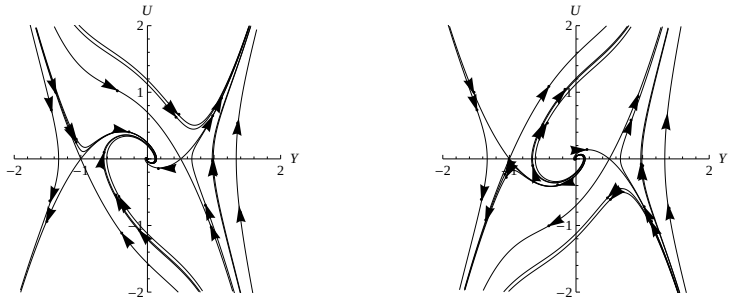

(a) $\alpha > 0$ (b) $\alpha < 0$

Figure 4.28: Changes in the case $\beta > \dfrac{\alpha^2}{4} > 0$, the origin is a spiral. ($f_2 = 1$, $g_2 = 2$, $\beta = 1$, $\alpha = \pm 1$).

II. At $(Y_2, 0)$, the Jacobian matrix is

$$A = \begin{pmatrix} 0 & 1 \\ \dfrac{f_2^2 + 4g_2\beta - f_2\sqrt{f_2^2 + 4g_2\beta}}{2g_2} & -\alpha \end{pmatrix}. \tag{4.83}$$

Therefore

$$\tau = -\alpha,\ \Delta = -\frac{f_2^2 + 4g_2\beta - f_2\sqrt{f_2^2 + 4g_2\beta}}{2g_2}. \tag{4.84}$$

In this case $\Delta \neq 0$.

(a) If $\Delta < 0$, then $(Y_2, 0)$ is a **saddle point**.

(b) If $\Delta > 0$, for $\alpha = 0$, $(Y_2, 0)$ is a **centre**.

However, for $\alpha \neq 0$, the point is stable when $\alpha > 0$, and unstable when $\alpha < 0$. Note that

$$\tau^2 - 4\Delta = \alpha^2 + \frac{2\left(f_2^2 + 4g_2\beta - f_2\sqrt{f_2^2 + 4g_2\beta}\right)}{g_2}. \tag{4.85}$$

i. If $\tau^2 - 4\Delta > 0$, then $(Y_1, 0)$ is a **node**.

ii. If $\tau^2 - 4\Delta < 0$, then we have **spiral node**.

iii. If $\tau^2 - 4\Delta = 0$, then $(Y_2, 0)$ is a linear degenerate node. We have solved the system numerically to get the behaviour of the nonlinear analysis.

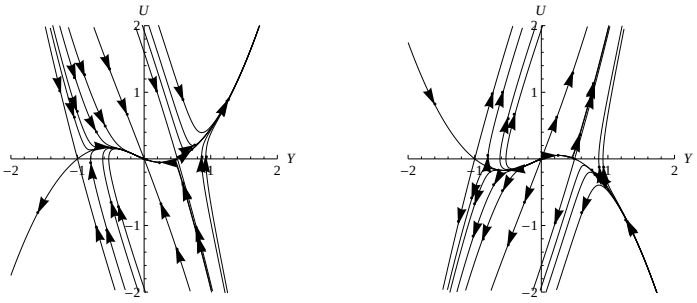

(a) $\alpha > 0$ (b) $\alpha < 0$

Figure 4.29: Changes in the case $0 < \beta < \dfrac{\alpha^2}{4}$, the origin is a node. ($f_2 = 1$, $g_2 = 2$, $\beta = 1$, $\alpha = \pm 3$).

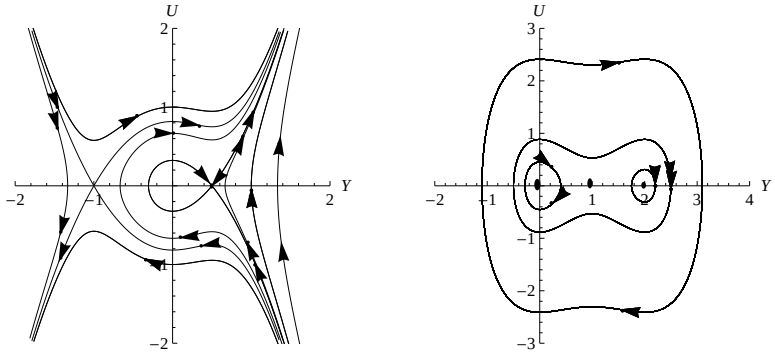

(a) (b)

Figure 4.30: Change in the case $\beta > 0$ and $\alpha = 0$, we have a centre at the origin. ($f_2 = 1$, $g_2 = 1$, $\beta = 1$ for (a), and $f_2 = 3$, $g_2 = -1$, $\beta = 2$ for (b)).

Since the analysis at the equilibrium points presents many different cases, we have just depicted some of the behaviour of the system using different values of β. We can visualise the changes of the behaviour in Figures 4.28 to 4.33.

3. If $f_2^2 + 4g_2\beta > 0$ and $\beta = 0$, i.e., $f_2 \neq 0$, from (4.75)–(4.77), we have two equilibrium points, $(0, 0)$ and $\left(-\dfrac{f_2}{g_2}, 0\right)$.

   I. At $(0, 0)$, the Jacobian matrix is given by

$$A = \begin{pmatrix} 0 & 1 \\ 0 & -\alpha \end{pmatrix}. \tag{4.86}$$

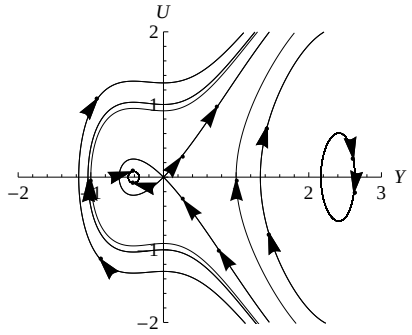

Figure 4.31: $\beta < 0$ and $\alpha = 0$: the system predicts a saddle point at the origin. ($f_2 = 2$, $g_2 = -1$, $\beta = -1$).

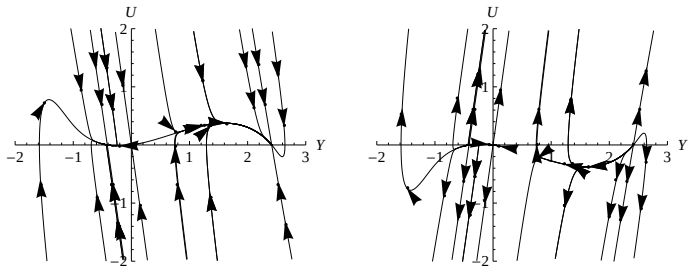

(a) $\alpha > 0$ (b) $\alpha < 0$

Figure 4.32: $\beta < 0$ and $\alpha \neq 0$: the system (4.19) predicts a saddle point at the origin. ($f_2 = 2$, $g_2 = -1$, $\beta = -1$, $\alpha = \pm 7$).

Thus $\tau = -\alpha$ and $\Delta = 0$. We are in a borderline case. As previously done, we have simulated the full system numerically to show the possible behaviour at this point. The results are incorporated into the diagrams for $\left(-\frac{f_2}{g_2}, 0\right)$.

II. At $\left(-\frac{f_2}{g_2}, 0\right)$, the Jacobian matrix given by

$$A = \begin{pmatrix} 0 & 1 \\ \frac{f_2^2}{g_2} & -\alpha \end{pmatrix} \tag{4.87}$$

yields $\tau = -\alpha$ and $\Delta = -\frac{f_2^2}{g_2}$ (which cannot be zero).

(a) If $g_2 > 0$, then $\Delta < 0$. Therefore we have a **saddle point**. The phase portrait is shown in Figure 4.34(a).

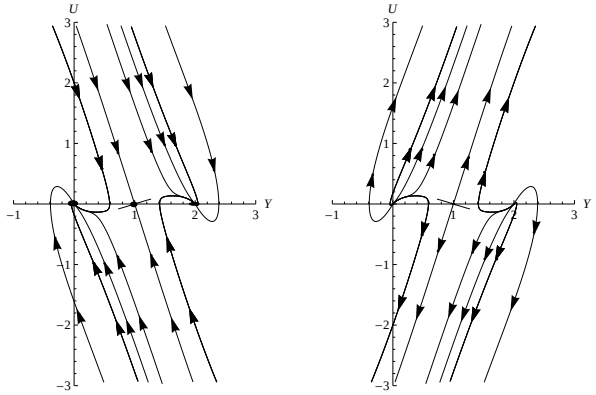

(a) stable node at $(0,0)$ (b) unstable node at $(0,0)$

Figure 4.33: Linear degenerate nodes at the equilibrium points predict by (4.19) ($f_2 = 3$, $g_2 = -1$, $\beta = 2$, $\alpha = \pm\sqrt{8}$).

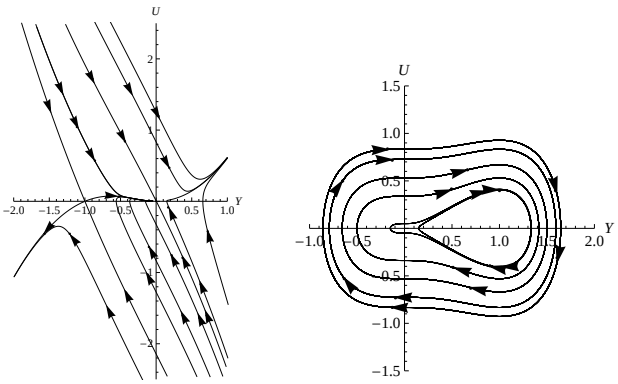

(a) (b)

Figure 4.34: The system (4.19) predicts (in the case where $f_2 \neq 0$ and $\beta = 0$) at $\left(-\frac{f_2}{g_2}, 0\right)$ a saddle point when $g_2 > 0$ ($f_2 = 1$, $g_2 = 1$, $\alpha = 2$), and a centre when $g_2 < 0$ and $\alpha = 0$ ($f_2 = 1$, $g_2 = -1$, $\alpha = 0$).

(b) If $g_2 < 0$, then $\Delta > 0$. For $\alpha = 0$, we have a **centre** (see Figure 4.34(b)).

However, for $\alpha \neq 0$, note that $\tau^2 - 4\Delta = \alpha^2 + \frac{4f_2^2}{g_2}$. The point is **stable** when $\alpha > 0$, and **unstable** when $\alpha < 0$.

i. If $\alpha^2 > -\frac{4f_2^2}{g_2}$, then the point is a **node** (see Figure 4.35).

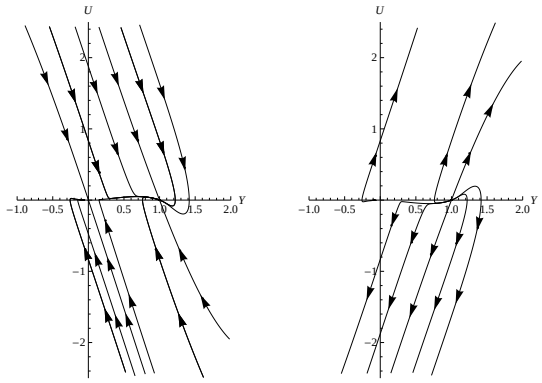

(a) (b)

Figure 4.35: Node at $\left(-\frac{f_2}{g_2}, 0\right)$ predicted by (4.19) when $\alpha^2 > -\frac{4f_2^2}{g_2}$ ($f_2 = 1$, $g_2 = -1$, $\alpha = \pm 3$).

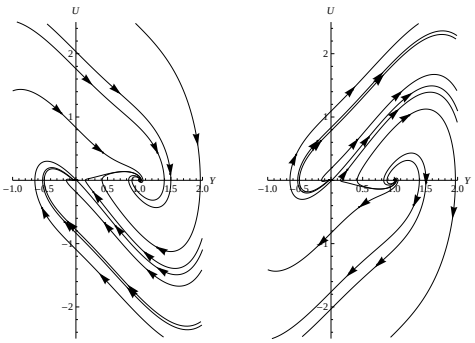

(a) (b)

Figure 4.36: Spiral at $\left(-\frac{f_2}{g_2}, 0\right)$ predicted by (4.19) when $\alpha^2 < -\frac{4f_2^2}{g_2}$ ($f_2 = 1$, $g_2 = -1$, $\alpha = \pm 1$).

ii. If $\alpha^2 < -\frac{4f_2^2}{g_2}$, we have a **spiral** (see Figure 4.36).

iii. If $\alpha^2 = -\frac{4f_2^2}{g_2}$, then the origin is a linear **degenerate node**. As in the other cases, we simulated the full system numerically to get the behaviour as shown in Figure 4.37.

4. If $f_2^2 + 4g_2\beta = 0$, i.e, $\beta = -\frac{f_2^2}{4g_2}$, from (4.76)-(4.77) we can say that we have two equilibrium points $(0, 0)$ and $\left(-\frac{f_2}{2g_2}, 0\right)$ for $\beta \neq 0$, and only one, the origin, for $\beta = 0$.

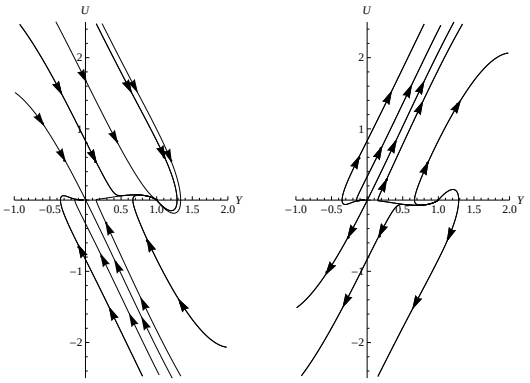

(a) $\alpha > 0$ (b) $\alpha < 0$

Figure 4.37: Changes of the system when $\alpha^2 = -\dfrac{4f_2^2}{g_2}$ ($f_2 = 1$, $g_2 = -1$, $\alpha = \pm 2$).

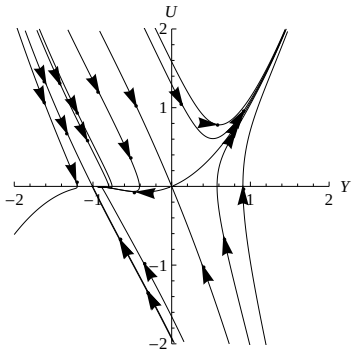

Figure 4.38: The system (4.19) predicted in the case where $f_2^2 + 4g_2\beta = 0$, $g_2 > 0$ and $\beta \neq 0$, a saddle point at the origin ($f_2 = 2$, $g_2 = 1$, $\beta = -1$, $\alpha = 2$).

I. At $\left(-\dfrac{f_2}{2g_2}, 0\right)$, the Jacobian matrix given by

$$A = \begin{pmatrix} 0 & 1 \\ 0 & -\alpha \end{pmatrix} \tag{4.88}$$

yields $\tau = -\alpha$ and $\Delta = 0$. This is a borderline case, so the possible phase portrait is obtained by doing a numerical simulation.

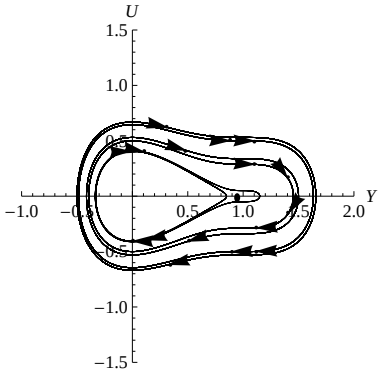

Figure 4.39: The system (4.19) predicted in the case $f_2^2 + 4g_2\beta = 0$, $g_2 < 0$, $\beta \neq 0$ and $\alpha = 0$, a centre at the origin ($f_2 = 2$, $g_2 = -1$, $\beta = 1$).

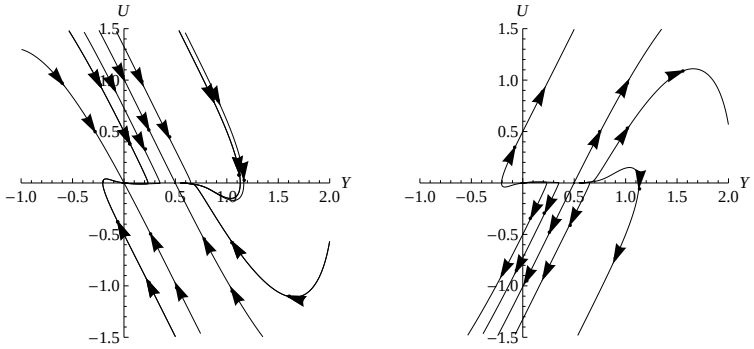

(a) Stable node (b) Unstable node

Figure 4.40: Node at the origin predicted by the system ($f_2 = 1$, $g_2 = -1$, $\beta = 0.25$, $\alpha = \pm 2$).

II. At the origin, the Jacobian matrix is given by

$$A = \begin{pmatrix} 0 & 1 \\ \dfrac{f_2^2}{4g_2} & -\alpha \end{pmatrix}. \tag{4.89}$$

Thus $\tau = -\alpha$ and $\Delta = -\dfrac{f_2^2}{4g_2}$.

(a) If $g_2 > 0$ and $\beta \neq 0$, then $\Delta < 0$. Therefore the origin is a **saddle point**. The phase portrait is shown in Figure 4.38.

(b) If $g_2 < 0$ and $\beta \neq 0$, then $\Delta > 0$. For $\alpha = 0$, we have a **centre** (see Figure 4.39).

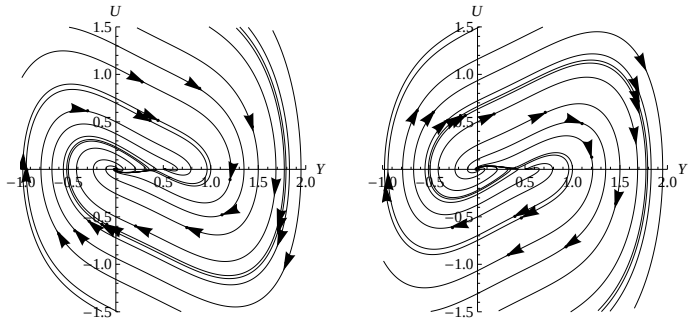

(a) Stable spiral (b) Unstable spiral

Figure 4.41: Spirals predicted at the origin ($f_2 = 1$, $g_2 = -1$, $\beta = 0.25$, $\alpha = \pm 0.5$).

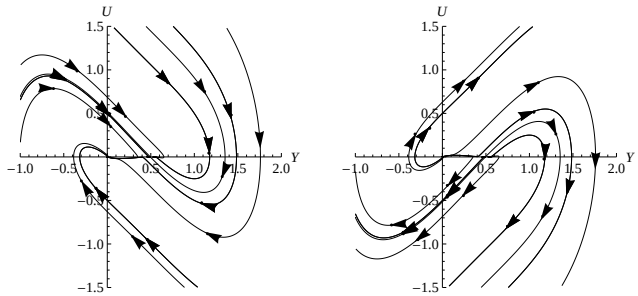

(a) Stable node (b) Unstable node

Figure 4.42: Degenerate node at the origin obtained after simulation of the system ($f_2 = 1$, $g_2 = -1$, $\beta = 0.25$, $\alpha = \pm 1$).

However, for $\alpha \neq 0$, note that $\tau^2 - 4\Delta = \alpha^2 + \dfrac{f_2^2}{g_2}$. In this case, the origin is **stable** when $\alpha > 0$, and **unstable** when $\alpha < 0$.

i. If $\alpha^2 > -\dfrac{f_2^2}{g_2}$, then the origin is a **node**. The behaviour is shown in Figure 4.40.

ii. If $\alpha^2 < -\dfrac{f_2^2}{g_2}$, we have a **spiral** (see Figure 4.41).

iii. If $\alpha^2 = -\dfrac{f_2^2}{g_2}$, then the origin is a linear **degenerate node**. Since we cannot extrapolate to the nonlinear case, we just simulate the system (see Figure 4.42).

(c) If $\beta = 0$, then $f_2 = 0$ and $\Delta = 0$. The origin is the only equilibrium point. Since we are in a borderline case, we simulated the system numerically to show the possible behaviour as shown in Figure 4.43.

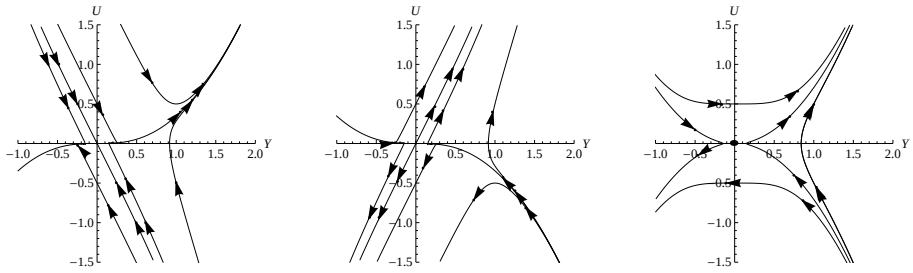

(a) $\alpha > 0$ (b) $\alpha < 0$ (c) $\alpha = 0$

Figure 4.43: Behaviour of the system (4.19) in the case where $\beta = 0$ and $f_2 = 0$.

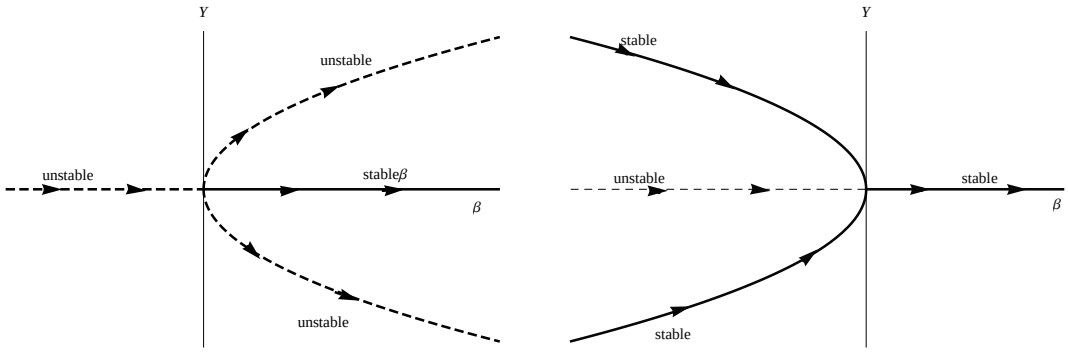

(a) supercritical bifurcation (b) subcritical bifurcation

Figure 4.44: Bifurcation diagram in charged fluid ($g_2 = \pm 1$).

From (4.75)–(4.77), a pitchfork bifurcation could occur, provided $f_2 = 0$ and $\alpha < 0$ (all the equilibrium points are unstable when $\alpha > 0$, and there is no change of stability).

Thus for $g_2 > 0$, when $\beta \leq 0$ the origin is the only equilibrium point, and is unstable. Two unstable equilibrium points appear in symmetrical pairs when $\beta > 0$, and the origin becomes stable (from (4.79)). There is a **supercritical pitchfork bifurcation**.

However, for $g_2 < 0$, when $\beta < 0$ there are three equilibrium points. The origin is unstable whereas the other two are stable (from (4.84)). When $\beta = 0$, the symmetrical pair points disappear but the origin remains unstable, and when $\beta > 0$ the origin becomes stable. In this case there is a **subcritical pitchfork bifurcation**, with β as the bifurcation parameter (g_2 cannot be a bifurcation parameter since it is different to zero). We can see the bifurcation diagrams in Figures 4.44(a)–4.44(b).

Chapter 5

Conclusion

5.1 Summary

In this dissertation we investigated the possible links between dynamical systems analysis and Lie symmetry analysis of ordinary differential equations. We undertook the investigation based on the equations

$$Y'' + \alpha Y' + \left(M + \frac{\alpha^2}{4}\right) Y = g_2 Y^3 + f_2 Y^2 + N, \tag{5.1}$$

and

$$Y'' + \alpha Y' + \beta Y = g_2 Y^3 + f_2 Y^2, \tag{5.2}$$

obtained by Kweyama *et al* [15] in the study of the behaviour of spherically symmetric charged fluids in general relativity. The Lie symmetry analysis led Kweyama *et al* [15] to obtain only one symmetry

$$G = \frac{\partial}{\partial X} \tag{5.3}$$

which does not achieve solutions of equations (5.1) and (5.2). Thereafter, they found some constraints (on parameters) for which (5.1) and (5.2) admit an additional symmetry, and became integrable. We were therefore interested to investigate the impact of those constraints on the qualitative behaviour of the equations.

In Chapter 1 we presented the use of Lie symmetry analysis and dynamical systems analysis

for differential equations. We also presented some simple known models of applications of dynamical systems analysis in one dimensional flow.

In Chapter 2 we gave an overview of dynamical systems analysis for two-dimensional flow. We began with linear systems by classifying the stability of equilibrium points, and then we extended the analysis to nonlinear systems. We also introduced local bifurcations, and illustrated them with examples.

In Chapter 3 we briefly outlined the algorithm to find the symmetries of nth order ordinary differential equations. The concept of Lie algebras was introduced which is crucial for the reduction of order.

In Chapter 4 we conducted a general dynamical system analysis of equations (5.1) and (5.2). Possible bifurcations were explored. For the borderline cases, we just solved the nonlinear system numerically to show the change of behaviour.

5.2 Impact of parameter values

In Chapter 4 we provided the general qualitative behaviour for (5.1) (when $g_2 = 0$ and $f_2 \neq 0$) and for (5.2) (when $g_2 \neq 0$, and when $g_2 = 0$ and $f_2 \neq 0$). For these cases Kweyama *et al* [15] provided special values of some parameters which allowed for an additional symmetry. We consider the implication of those parameters on our qualitative analysis.

1. Consider equation (5.1) in the neutral perfect fluid case ($g_2 = 0$ and $f_2 \neq 0$). Kweyama *et al* [15] obtained (when $\alpha \neq 0$) the additional symmetry

$$G_2 = e^{(\alpha/5)X}\frac{\partial}{\partial X} + e^{(\alpha/5)X}\left(-\frac{2\alpha}{5}Y + \frac{\alpha M}{5f_2} + \frac{\alpha^3}{500f_2}\right)\frac{\partial}{\partial Y}, \tag{5.4}$$

provided

$$N = \frac{M^2}{4f_2} + \frac{M\alpha^2}{8f_2} + \frac{49\alpha^4}{40000f_2}. \tag{5.5}$$

From §4.1.2 this parameter value for N belongs to the region where $16M^2 - 64f_2N + 8M\alpha^2 + \alpha^4 > 0$, but it is not a critical value in terms of the behaviour of the system. The stability analysis shows two steady states: one at $\left(\frac{M}{2f_2} + \frac{49\alpha^2}{200f_2}, 0\right)$ which is a **saddle**

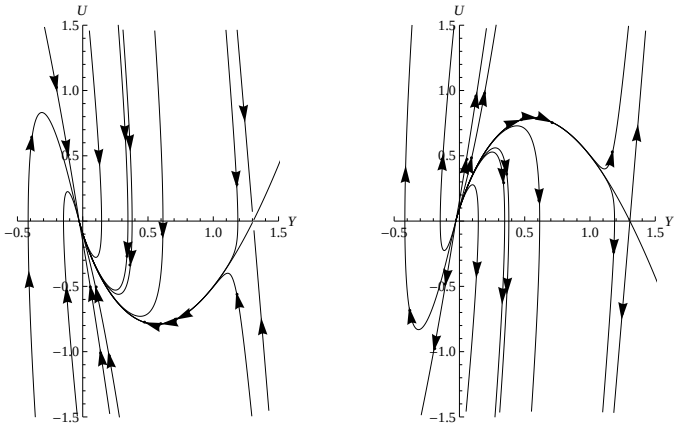

(a) Stable node, saddle point

(b) saddle point, unstable node

Figure 5.1: Behaviour of (5.1) in the neutral perfect fluid case when $\alpha \neq 0$ and $N = \frac{M^2}{4f_2} + \frac{M\alpha^2}{8f_2} + \frac{49\alpha^4}{40000f_2}$ ($f_2 = 18$, $\alpha = \pm 10$, $M = -2$).

point, and the other at $\left(\frac{M}{2f_2} + \frac{\alpha^2}{200f_2}, 0\right)$ which is a **node**. The node is **stable** if $\alpha > 0$, and is **unstable** if $\alpha < 0$. Here, there is no bifurcation. We can see the behaviour of the system as shown in Figures 5.1(a)–5.1(b).

2. (a) For equation (5.2), Kweyama *et al* [15] found when $f_2 \neq 0$ and $\alpha \neq 0$

$$G_2 = e^{(\alpha/3)X}\frac{\partial}{\partial X} - e^{(\alpha/3)X}\left(\frac{\alpha}{3}Y + \frac{2\alpha^3}{9f_2}\right)\frac{\partial}{\partial Y} \tag{5.6}$$

as an additional symmetry, provided the following conditions apply:

$$\beta = -\frac{4\alpha^2}{9}, \quad g_2 = \frac{f_2^2}{2\alpha^2}. \tag{5.7}$$

From §4.2.2 the parameters g_2 and β in (5.7) are not special – they do not change the stability of the system, but they correspond to the region where $f_2^2 + 4g_2\beta > 0$ and $\beta \neq 0$. In this region we have three equilibrium points: $(0,0)$ and $\left(-\frac{4\alpha^2}{3f_2}, 0\right)$ which are **saddle points**, and $\left(-\frac{2\alpha^2}{3f_2}, 0\right)$ which is a **node**. The node is **stable** when $\alpha > 0$, and **unstable** when $\alpha < 0$ (see Figures 5.2(a)–5.2(b)).

(b) When $f_2 = 0$ ($g_2 \neq 0$), Kweyama *et al* [15] found

$$G_2 = e^{(\alpha/3)X}\frac{\partial}{\partial X} - \frac{\alpha}{3}e^{(\alpha/3)X}Y\frac{\partial}{\partial Y} \tag{5.8}$$

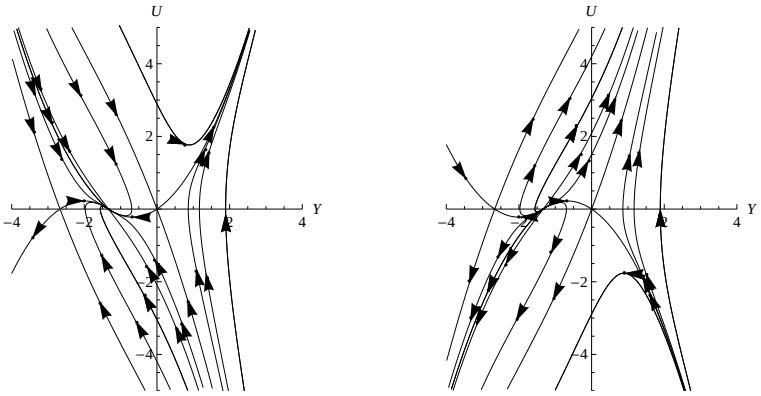

(a) $\alpha > 0$ (b) $\alpha<0$

Figure 5.2: Behaviour of (5.2) in the charged fluid, with $f_2 \neq 0$ ($f_2 = 2$, $\alpha = \pm 2$).

as an additional symmetry, provided

$$\beta = \frac{2\alpha^2}{9}. \tag{5.9}$$

In this case β is also not special. Note that $f_2^2 + 4g_2\beta = \frac{8}{9}g_2\alpha^2$.

i. If $g_2 > 0$ and $\alpha \neq 0$, then $f_2^2 + 4g_2\beta > 0$. Thus from §4.2.2 we have three equilibrium points: $(0,0)$, $\left(\frac{\sqrt{2}\alpha}{3\sqrt{g}}, 0\right)$ and $\left(-\frac{\sqrt{2}\alpha}{3\sqrt{g}}, 0\right)$. The stability analysis shows that the origin is a **node** (because $0 < \beta < \frac{\alpha^2}{4}$), whereas the two others points are **saddle points**. The node is **stable** when $\alpha > 0$, and **unstable** when $\alpha < 0$. The behaviour is shown in Figures 5.3(a)–5.3(b).

ii. If $g_2 < 0$ and $\alpha \neq 0$, then $f_2^2 + 4g_2\beta < 0$. Therefore, from §4.2.2 the only equilibrium point, the origin, is a **node** (since $0 < \beta < \frac{\alpha^2}{4}$). The node is **stable** when $\alpha > 0$, and **unstable** when $\alpha < 0$ (see Figures 5.4(a)–5.4(b)).

iii. When $\alpha = 0$, the origin is again the only equilibrium point, and at that point, the determinant $\Delta = 0$. This is a borderline case. The behaviour has been obtained in §4.2.2 by simulating the system numerically, as shown in Figure 5.4(c).

3. Consider equation (5.2) in the neutral perfect fluid case ($g_2 = 0$ and $f_2 \neq 0$). Maharaj *et*

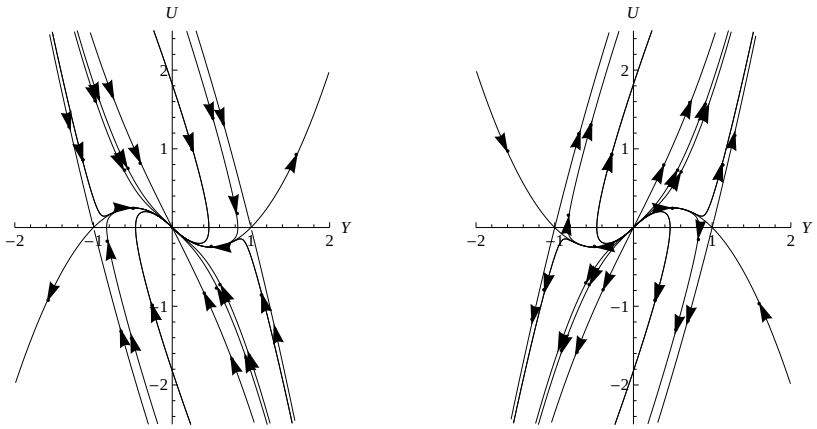

(a) Stable node at $(0,0)$ (b) Unstable node at$(0,0)$

Figure 5.3: Behaviour of (5.1) in the charged fluid when $f_2 = 0$, $g_2 > 0$ and $\alpha \neq 0$. The system predicts node and saddle points ($g_2 = 2$ and $\alpha = \pm 3$).

al [16] obtained an additional symmetry subject to the condition

$$\beta = \pm\frac{6\alpha^2}{25}. \tag{5.10}$$

The analysis in this case corresponds to the one in §4.1.2 (with $M = \beta - \dfrac{\alpha^2}{4}$ and $N = 0$). The value of β is not special.

(a) When $\alpha = 0$, then $\beta = 0$. Thus from §4.1.2 the origin is the only equilibrium point (since $M^2 - 4f_2N = 0$), and at that point the trace $\tau = 0$ and the determinant $\Delta = 0$. We simulate the system numerically to obtain the behaviour as shown in Figure 5.5(a).

(b) When $\alpha \neq 0$, consider $\beta = \dfrac{6\alpha^2}{25}$. Since $16M^2 - 64f_2N + 8M\alpha^2 + \alpha^4 > 0$, from §4.1.2 we have two equilibrium points, $(0,0)$ and $\left(\dfrac{6\alpha^2}{25f_2}, 0\right)$. The stability analysis showed that the origin is a **node**, and $\left(\dfrac{6\alpha^2}{25f_2}, 0\right)$ is a **saddle point**. The node is **stable** when $\alpha > 0$, and **unstable** when $\alpha < 0$ (See Figures 5.5(b)–5.5(c)).
However, for $\beta = -\dfrac{6\alpha^2}{25}$, our equilibrium points are $(0,0)$ which is **saddle point**, and $\left(-\dfrac{6\alpha^2}{25f_2}, 0\right)$ which is a **node** (see Figures 5.6(a)–5.6(b)).

We observe that the system behaves differently depending on the sign of β in (5.10).

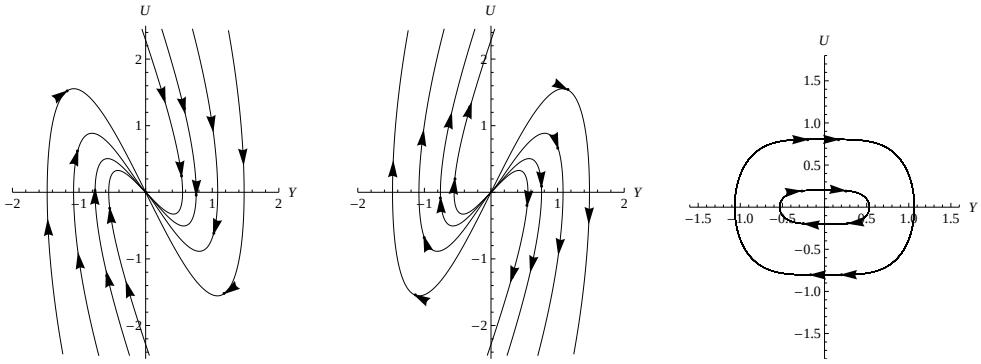

(a) $g_2 < 0$ and $\alpha > 0$ (b) $g_2 < 0$ and $\alpha < 0$ (c) $\alpha = 0$

Figure 5.4: Behaviour of (5.1) in the charged fluid when $f_2 = 0$. The system predicts a node when $g_2 < 0$ and $\alpha \neq 0$, and a centre when $\alpha = 0$ ($g_2 = -2$ and $\alpha = \pm 3$).

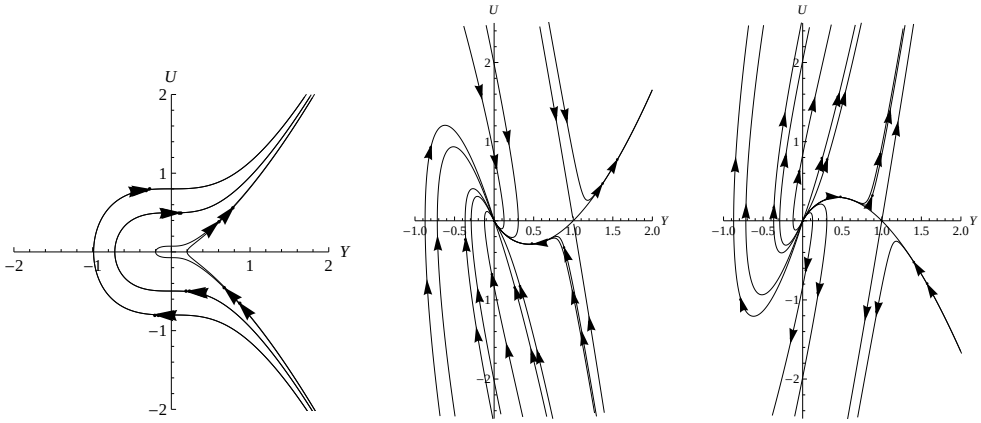

(a) $\alpha = 0$ (b) $\alpha > 0$ (c) $\alpha < 0$

Figure 5.5: Behaviour of (5.2) in the neutral perfect fluid when $\beta = \dfrac{6\alpha^2}{25}$. The system predicts for $\alpha = 0$ a cusp ($f_2 = 1$), and for $\alpha \neq 0$ a node and a saddle point ($f_2 = 6$, $\alpha = \pm 5$).

5.3 Discussion

In view of the foregoing, we observe that the constraints obtained by Kweyama *et al* [15] in their quantitative study, do not fully integrate with our qualitative study. The special values obtained via the Lie symmetry analysis are not special when it comes to the dynamical systems

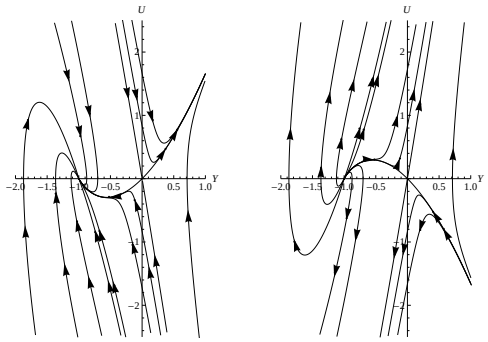

(a) (b)

Figure 5.6: Behaviour of (5.2) in the neutral perfect fluid when $\beta = -\dfrac{6\alpha^2}{25}$. For $\alpha \neq 0$, the system predicts a node and a saddle point ($f_2 = 6$, $\alpha = \pm 5$).

analysis, and with these values there is no bifurcation.

However, in §4.1.3 (where $16f_2^2 + 48g_2M + 12g_2\alpha^2 > 0$) it was difficult, even impossible, to pursue the stability analysis of the system, because the equilibrium points were complicated and there was no way to isolate the real values. In this case, we used the corresponding constraints obtained by Kweyama *et al* in the Lie symmetry analysis to pursue our dynamical systems analysis and obtain the local behaviour of the system.

Therefore we can use the dynamical system analysis to test the relevance of symmetries, and of solutions (for example, special solutions or not) obtained from the Lie symmetry analysis. We can also predict the stability of the solutions, even possible bifurcations. On the other hand, in certain robust case of qualitative analysis, we can use Lie symmetry analysis to investigate constraints that will enable us to study the system locally. Thus we conclude and advise that it is quite important to together utilise both techniques of analysis.

Bibliography

[1] Adhikari M. R. and Adhikari A., *Text Book of Linear Algebra: An Introduction to Modern Algebra* (Allied, New Delhi, 2004)

[2] Andronov A. A., Leontovich E. A., Gordon I. J. and Maier A. G., *Theory of Bifurcations of Dynamical Systems on a Plane* (Wiley, New York, 1973)

[3] Åström K. J. and Murray R. M., *Feedback Systems: An Introduction for Scientists and Engineers* (Princeton University Press, Woodstock, 2008)

[4] Blanchard P., Devaney R. L., and Hall G. R., *Differential Equations* (Brooks-Cole, California, 1998)

[5] Bluman G. W. and Anco S. C., *Symmetry and Integration Methods for Differential Equations*, Applied Mathematical Sciences **154** (Springer-Verlag, New York, 2002)

[6] Britton N. F., *Essential Mathematical Biology* (Springer-Verlag, London, 2003)

[7] Clark A., DynPac (version 11.03): A Dynamical Systems Package for Mathematica 7 (New York, 2009)

[8] Das B. M., *Theoretical Foundation Engineering* (J. Ross, Fort Lauderdale, 2007)

[9] Girimaji S. S., Langley Research Center, *Dynamical System Analysis of Reynolds Stress Closure Equations* (NASA/CR-201749, Hampton, 1997)

[10] Guckenheimer J. and Holmes P., *Nonlinear Oscillations, Dynamical Systems, and Bifurcations of Vectors Fields*, Applied Mathematical Sciences **42** (Springer-Verlag, New York, 1983)

[11] Hydon P. E., *Symmetry Methods for Differential Equations. A Beginner's Guide* (Cambridge University Press, Cambridge, 2000)

[12] Ibragimov N. H., *CRC Handbook of Lie Group Analysis of Differential Equations: Symmetries, Exact Solutions and Conservation Laws* **1** (CRC Press, Boca Raton, 1994)

[13] Irving R. S., *Integers, Polynomials, and Rings: A Course in Algebra* (Springer-Verlag, New York, 2004)

[14] Jacobson M. J., Jr, Williams H. C., *Solving the Pell Equation* (Springer-Verlag, New York, 2009)

[15] Kweyama M. C., Govinder K. S., and Maharaj S. D, *Noether and Lie symmetries for charged perfect fluids*, Class. Quantum Grav. **28** (2011) 1–13

[16] Maharaj S. D., Leach P. G., and Maartens R., *Expanding Spherically Symmetric Models without Shear*, Gen. Rel. Grav. **28** (1996) 35–50

[17] Mahomed F. M. and Leach P. G., *Symmetry Lie algebras of nth order ordinary differential equations*, J Math Anal. Appl. **151** (1990) 80-107

[18] Maplesoft, *Maple version 15.01* (Waterloo, 2011)

[19] Murray J. D., *Mathematical Biology I. An Introduction*, Interdisciplinary Applied Mathematics **17** (Springer-Verlag, Berlin, 2002)

[20] Olver P. J., *Applications of Lie Groups to Differential Equations* (Springer-Verlag, New York, 1993)

[21] Perko L., *Differential Equations and Dynamical Systems* (Springer-Verlag, New York, 1991)

[22] Procesi C., *An Approach through Invariants and Representations* (Springer Science+Business Media, New York, 2007)

[23] Scheinerman E. R., *Invitation to Dynamical Systems* (Prentice Hall, New Jersey, 1996)

[24] Strogatz S. H., *Nonlinear Dynamics and Chaos with applications to Physic, Biology, Chemistry and Engineering* (Perseus Books, New York, 1994)

[25] Surhone L. M., Timpledon M. T. and Marseken S. F., *Saddle-Node Bifurcation* (VDM Verlag Dr. Mueller AG & Co. Kg, Beau Bassin, 2010)

[26] Wolfram Research, Inc., *Mathematica version 7* (Wolfram Research, Urbana-Champaign, 2008)